Journal of
Manufacturing and Materials Processing

MDPI

Review

Liquid-Based 4D Printing of Shape Memory Nanocomposites: A Review

Mohamad Alsaadi [1,2,3,*], Eoin P. Hinchy [1,4], Conor T. McCarthy [1,4], Vicente F. Moritz [2], Shuo Zhuo [2], Evert Fuenmayor [2,5] and Declan M. Devine [2]

1 Confirm Centre for Smart Manufacturing, University of Limerick, V94 T9PX Limerick, Ireland
2 PRISM Research Institute, Technological University of the Shannon, N37 HD68 Athlone, Ireland
3 Materials Engineering Department, University of Technology, Baghdad 10066, Iraq
4 School of Engineering, University of Limerick, V94 T9PX Limerick, Ireland
5 Faculty of Engineering, Design and Informatics, Technological University of the Shannon, N37 HD68 Athlone, Ireland
* Correspondence: mohamad.alsaadi@ul.ie or mohamad.alsaadi@ait.ie

Abstract: Significant advances have been made in recent years in the materials development of liquid-based 4D printing. Nevertheless, employing additive materials such as nanoparticles for enhancing printability and shape memory characteristics is still challenging. Herein, we provide an overview of recent developments in liquid-based 4D printing and highlights of novel 4D-printable polymeric resins and their nanocomposite components. Recent advances in additive manufacturing technologies that utilise liquid resins, such as stereolithography, digital light processing, material jetting and direct ink writing, are considered in this review. The effects of nanoparticle inclusion within liquid-based resins on the shape memory and mechanical characteristics of 3D-printed nanocomposite components are comprehensively discussed. Employing various filler-modified mixture resins, such as nanosilica, nanoclay and nanographene, as well as fibrous materials to support various properties of 3D printing components is considered. Overall, this review paper provides an outline of liquid-based 4D-printed nanocomposites in terms of cutting-edge research, including shape memory and mechanical properties.

Keywords: additive manufacturing (AM); shape memory (SM); polymer nanocomposites; stereolithography (SLA); digital light processing (DLP); material jetting (MJ); direct ink writing (DIW)

Citation: Alsaadi, M.; Hinchy, E.P.; McCarthy, C.T.; Moritz, V.F.; Zhuo, S.; Fuenmayor, E.; Devine, D.M. Liquid-Based 4D Printing of Shape Memory Nanocomposites: A Review. *J. Manuf. Mater. Process.* **2023**, *7*, 35. https://doi.org/10.3390/jmmp7010035

Academic Editor: Giorgio De Pasquale

Received: 31 December 2022
Revised: 21 January 2023
Accepted: 25 January 2023
Published: 31 January 2023

1. Introduction

In recent years, shape memory polymers and their composites (SMPs/SMPCs) have attracted substantial attention due to ease of processing, lightweight properties and low cost compared to their metallic counterparts, namely shape memory alloys. SMPs are materials that can recover from temporarily induced deformations to their original shape. Most SMPs are chemically crosslinked (thermosets) or physically crosslinked (thermoplastics). The two stages of the shape memory effect (SME) for the SMPs are shape fixing (temporary shape) and shape recovery (permanent shape). Many conventional fabrication methods have been used to develop shape memory polymers. However, the need for complex geometric designs exhibiting shape memory behaviour has compelled researchers to ponder the compatibility of these materials with 3D printing fabrication methods, which offer leading production technology to achieve such designs. In accordance with the recent additive manufacturing (AM) standard ISO/ASTM 52900:2021 [1], there are different categories of AM technologies that can be used to fabricate shape memory components in order to employ them in various innovative applications (Figure 1). Therefore, 3D printing (3DP) publications of shape memory polymers have rapidly increased in the last ten years (Figure 2). The shape memory polymer market size was USD 450 million in 2021, and it is forecast to grow by 2030 to become around USD 3.5 billion, driven by the growing product

demand in the automotive, aerospace, etc., sectors using various polymeric materials, such as polyurethane, poly(vinyl chloride), acrylic and epoxy [2].

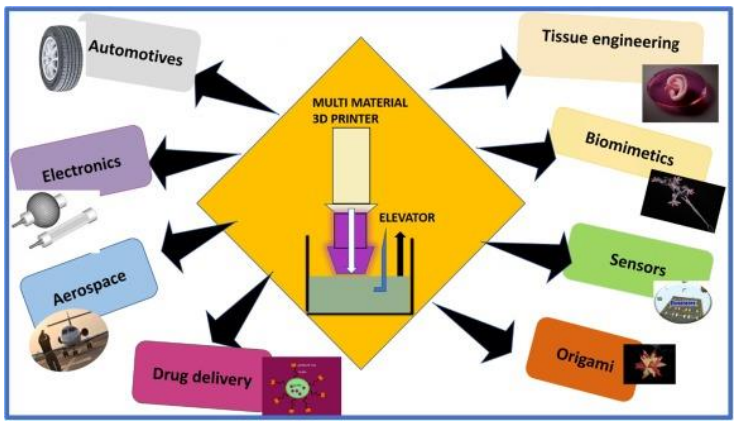

Figure 1. Applications for SMPs/SMPCs [2]. Copyright © 2022 Elsevier.

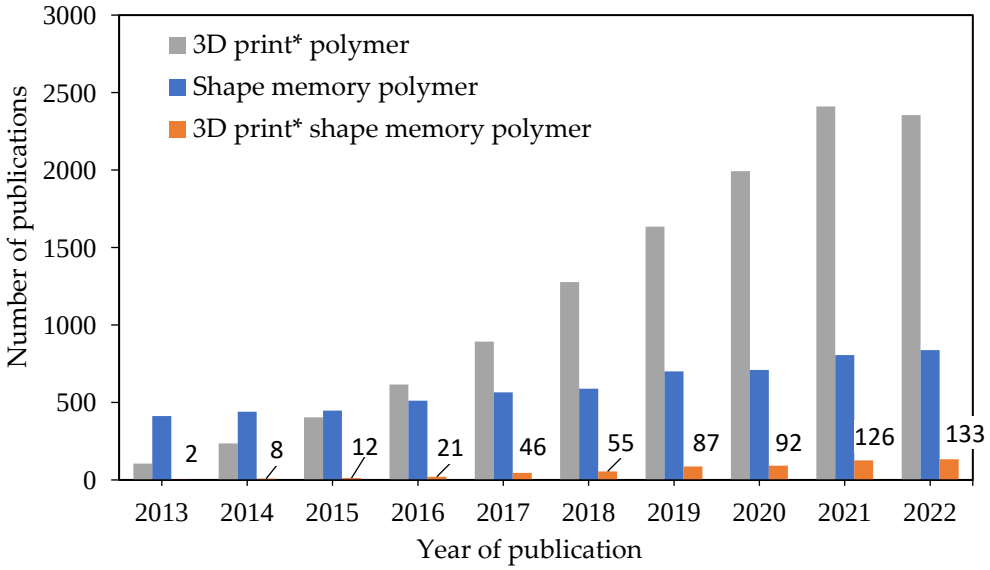

Figure 2. The number of publications related to 3DP of SMP since 2013 (data from Web of Science, 2022).

In essence, 4D printing (4DP) is a process by which 3D-printed components can be programmed to transform their shape over time when exposed to external stimuli. The 3D-printed component has only one static structure. In comparison, the 4D-printed smart component has at least two smart states, i.e., static and dynamic structures. The smart dynamic structure is activated by an external stimulus, triggering the shape and morphological transformations that can be effectively controlled and linked to macroscopic movements [3,4]. The smart component recovers its original shape in response to a specific stimulus depending on the requirements of end use, such as physical stimuli (thermosensitive [5], light-responsive [6], electrical/magnetic-responsive [7], etc.), chemical stimuli (moisture-responsive [8] and pH-responsive [9]) and biological stimuli (biomolecule-responsive) [10].

Liquid-based 3DP technology has received renewed interest by employing innovative polymeric resins. Liquid-based additive manufacturing technologies can be divided into three methods depending on the process of curing resin by the principle of building structure layer-by-layer polymerisation. These methods include (i) photopolymerisation, where the liquid precursor is crosslinked by UV or laser-light scanning; (ii) material jetting,

where the liquid resin is jetted onto a substrate, followed by UV curing right after; and (iii) DIW material extrusion, where the liquid resin with desired thixotropic rheology is extruded from a nozzle and deposited to form a 3D structure [11,12]. Recent developments have extended the materials manufacturing library thanks to the numerous advantages of photopolymerisation (also known as photocuring or photocrosslinking and mainly used for thermoset resins). Therefore, various 3D printers have been used, including stereolithography (SLA), digital light processing (DLP), continuous liquid interface printing (CLIP), two-photon absorption (TPA), liquid crystal display (LCD) and volumetric 3DP (V3DP) [13–16]. On the other hand, material jetting techniques, such as continuous ink jetting (CIJ) and drop-on-demand (DoD), have attracted significant attention due to several advantages for their printed components, such as multicolour materials, good surface finish, high dimensional accuracy and homogeneous mechanical properties [17–20]. Further, the material extrusion technique, i.e., DIW, has emerged as the most versatile 3DP technique for the broadest range of materials [21–23]. Figure 3 presents the liquid-based 3D printing methods and their materials' shape memory characteristics.

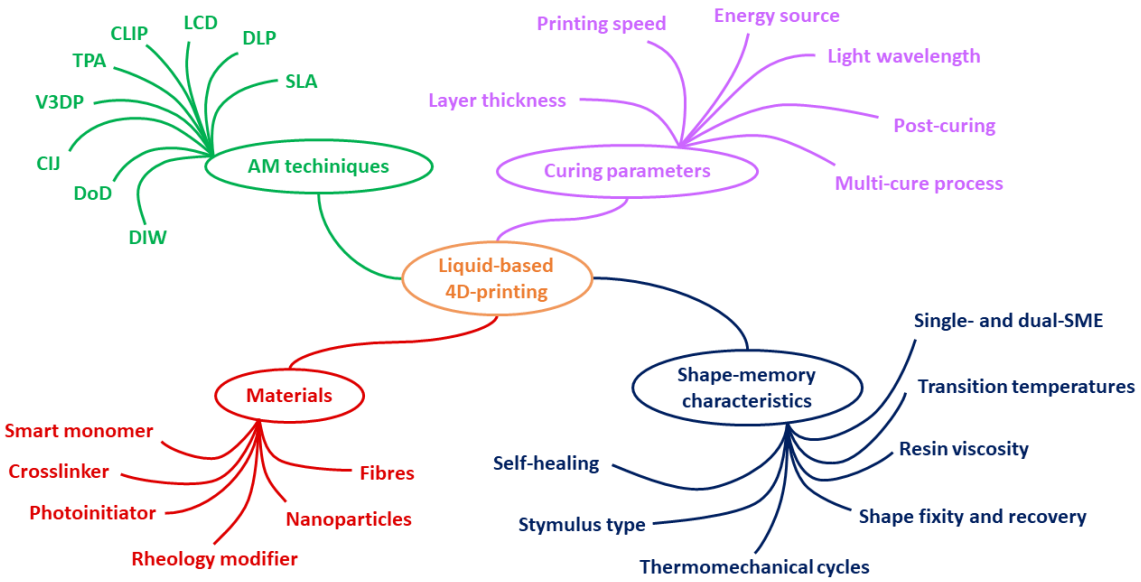

Figure 3. Liquid-based 3D printing of shape memory polymers.

The photopolymerisation method transforms the liquid monomer into a solid polymer via a light-curable reaction with the presence of a photoinitiator. The photoinitiator is a light-sensitive material that can absorb UV light and convert photolytic energy to create an active species that reacts with the monomers to initiate polymer chain growth [24]. There are several benefits for photopolymerisation compared to conventional polymerisation, such as less energy consumption (lower reaction temperature), reduced waste and fast curing under mild conditions (even at room temperature). In addition, photopolymerisation technology is considered to have low energy consumption and, thus, is friendly for the environment [25,26]. In general, there are two methods of photochemical photoinitiator-initiated polymerisation, namely radical and cationic; every technique has limitations and benefits [27,28].

The material jetting (MJ) method drops the photopolymer resin over a selected area by exposing it to UV light as a curing technique to produce a layer. It can be either jetted with resin when required (DoD) or utilise continuous jetting (CIJ) in accordance with the component shape [19]. MJ 3DP has a unique fabrication process that brings high speed and accuracy together in a multicolour, multi-material process in printing liquid-based components [29]. The main parts of the material jetting 3D printer are print heads, UV light sources, build platform, levelling blade and material containers. Many materials

can be used in jetting techniques, such as casting wax, thermoplastic, thermosetting and elastomeric polymers [20,30].

Direct ink writing is a material extrusion technique that uses materials, such as monomers/oligomers, crystal/silicone elastomers, crosslinkers and fillers. The most critical issue facing DIW 3DP is modified ink's rheology to be printable thixotropic fluid; this modification can be achieved by incorporating additives such as nanoparticles. In addition, DIW requires the material to be shear thinned for extrusion through a fine nozzle and maintain its shape after extrusion.

However, finding a compatible liquid-based resin to fabricate 3D-printed components having good shape memory, mechanical and thermal characteristics is still a substantial challenge for researchers. This returns to the selection process for the monomer/oligomer, initiator, additive, rheology modifier, polymerization type and power/wavelength of light [31,32]. A systematic review methodology aimed to investigate the growth in publications related to 4D printing in the last ten years. The data from relevant papers, i.e., research articles, review articles, conference articles, book chapters and case studies, were collected from different science citation-indexed journals using the keywords "3D print* shape memory polymer" and "4D printing" in the title, keywords and abstract. The research direction of this review aims to provide a comprehensive insight into the recent developments in liquid-based 4DP technologies and highlights novel 4D-printable polymeric resins and their nanocomposite components.

The organisation of this review paper is as follows: First, a general introduction on liquid-based 4DP and its technologies with an emphasis on SMPs is provided, followed by a detailed explanation on the working of liquid-based 3DP techniques. Then, the mechanisms of 4DP and SMP are described. Furthermore, materials for photopolymerisation, jetting and DIW extrusion techniques are comprehensively represented based on a literature review of the current work, which focuses on the effect of the inclusion of photoinitiator, nanoparticle and micro/nanofibre on the polymerisation process, shape memory properties and mechanical characteristics of the 3D-printed components. Finally, the conclusion and future scope in this review outline the challenges facing liquid-based 4DP technologies and their key solutions.

2. Liquid-Based 3DP Techniques

The evolution of additive manufacturing technologies has enabled the industry to develop complex-shape polymer-based parts for novel applications at lower costs [33–36]. Developed liquid resins are often used to fabricate smart components via a range of rapid prototyping methods based on photopolymerisation, material extrusion or material jetting techniques [35–39].

When employing additive manufacturing to build a part, it is crucial to keep in mind that the x- and y-axes are related to the build platform plane, while the z-axis corresponds to the axis of vertical motion of the build platform. Each part's layer may be understood as a set of coordinates (pixels) on a plane. Thus, the spatial resolution, i.e., related to x- and y-axes, arises from the building spot precision and accuracy, related to the AM technique's constructive process, whilst the resolution on the z-axis is mainly associated with the system's ability to control the vertical motion of the build platform [40–42].

This section will discuss the liquid-based 3D printer technologies, i.e., photopolymerisation, material jetting and DIW material extrusion techniques.

2.1. Photopolymerisation Techniques

The strategy of photopolymerisation is based on using liquid-state monomers/oligomers in the presence of a photoinitiator material, which can be polymerised via a photochemical reaction under radical, cationic or mixed-mode mechanisms during exposure to UV or laser irradiation, with a specific wavelength and curing depth [25,43]. In addition, some materials can be included in the mixture resin, such as a diluent/solvent, particle and fibre. The performance of the 3DP using the photopolymerisation technique

depends on the components, such as a light source, curing direction, build platform and resin tank. The light source can be xenon lamps, mercury arc lamps, LEDs or lasers. Several 3D printers use this technology in producing shape memory components, such as SLA, DLP, CLIP and LCD, which are discussed in this section [39,44].

2.1.1. Stereolithography (SLA)

The SLA technique builds a 3D part by focusing a UV laser on the photopolymerisable resin to link the molecule chains [40,45]. The apparatus consists of a vat containing liquid resin and a movable build platform (Figure 4). The conventional apparatus layout has a UV source, an *x*-*y* scanning mirror over the resin and a platform that moves downwards as the UV laser beam locally cures the resin, i.e., photopolymerises the resin layer by layer. The inverted layout has a UV-transparent window on the bottom of the vat, and the UV source and the *x*-*y* scanning mirror are placed under the vat, the build platform moving upwards as the resin is locally UV cured layer by layer [41,45,46]. The time required to print each layer relies on the UV laser beam speed and the irradiated area. These, in turn, are a consequence of a set of scanning mirrors, which reflect the laser beam along the *x*-*y* plane, photocuring the resin pixel by pixel, so that the surface of the photoreactive resin is sequentially exposed to the scanning laser beam [41,46]. When completing printing, the object is pulled out from the remaining resin in the vat. It is cleaned with a cleaning agent, e.g., isopropanol, to remove any unreacted resin and then is subjected to a UV post-curing stage to improve the part's final properties [40].

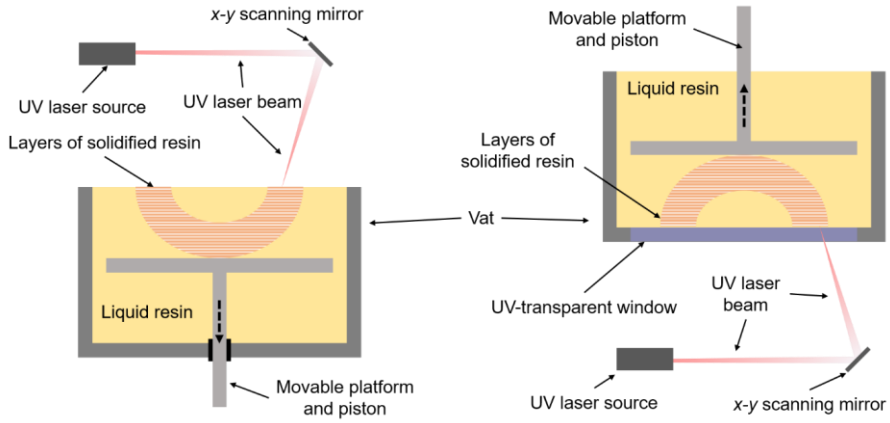

Figure 4. Schematic of a typical stereolithography printing method.

For instance, researchers have already demonstrated the effective use of liquid-based resins consisting of photoreactive liquid and fillers, such as silver nanoparticles, copper powder, halloysite nanoclay, montmorillonite and fibres, employing these materials for SLA 3D printing [47,48]. Furthermore, SLA has facilitated the advancement of 3D-printable stimuli-responsive materials, often utilising epoxy- and acrylate-based liquid resins [49–52] that contain fillers, such as preformed polymeric particles [50] or magnetic iron oxide nanopowder [53]. Variations of SLA, such as mask image projection-based stereolithography (MIP-SL), projection micro-stereolithography (PμSL) and two-photon polymerisation-based printing (2PP), have also been employed within this context [54–56].

2.1.2. Digital Light Processing (DLP)

The DLP technique is a variation of SLA and differs from the latter as it can irradiate each whole layer at once, through a selectively masked light source, instead of having a laser beam that operates on a pixel-by-pixel basis [46,57,58]. The equipment layout is very similar to an inverted SLA; however, instead of having scanning mirrors and a UV laser beam, there is a UV digital projector and a set of micro-mirrors (Figure 5) that can simultaneously irradiate each pixel, which allows for the whole layer to be exposed at a single step and to cure at the same time as well [46,57,58]. In this case, the time required to

print each layer does not depend on the area to be printed, and the overall process speed is higher than that of SLA. The usage of DLP technology for stimuli-responsive materials has already been reported in the literature [37,58–66].

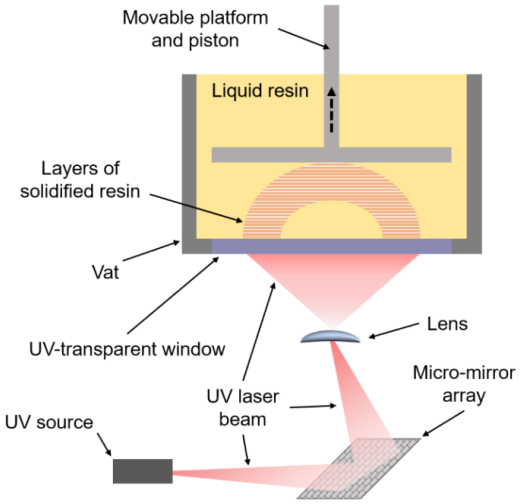

Figure 5. Schematic of a typical DLP printing method.

2.1.3. Continuous Liquid Interface Printing (CLIP)

CLIP arises as a development from the DLP system, having the same irradiation technology, but allowing the part to be built uninterruptedly with a continuous liquid surface, i.e., the build platform is constantly moving rather than stepwise, as in conventional vat photopolymerisation techniques (Figure 6). This behaviour leads to avoiding layer separation and recoating so that the printing process is claimed to be even faster, as there is no need to pause it between each printed layer [41,67–69]. The main advantage of CLIP is the polymerisation inhibition due to the oxygen content in the dead zone, causing the partially consumed reagents at the bottom region of the solid to behave like a living polymerisation system as the liquid interface is continuous [70,71].

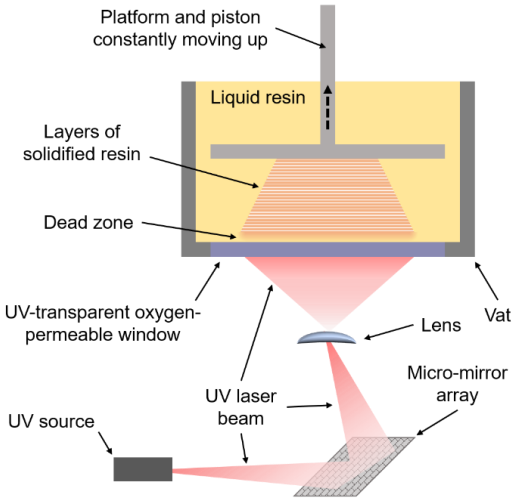

Figure 6. Schematic of a typical CLIP printing method.

In this method, the UV laser beam irradiates the bottom of the vat, projecting the cross-section of the part to be printed; the cross-section projection is continuous and changes progressively like a film instead of launching each layer at a specific time. The printed component is continually moved up, allowing enough time for the photosensitive monomers to react and for the liquid resin to flow underneath the last cured resin portion [72,73]. This

behaviour produces a "dead zone", i.e., a permanent liquid interface between the solid and the UV-transparent window, where, due to an oxygen-permeable membrane placed beneath the resin, the monomer is prevented from reacting as a consequence of the higher oxygen concentration [70,71]. Regarding liquid-based pastes, Ware and Sun (2019) reported the formulation of ceramic-loaded composite inks consisting of photoreactive resin and hydroxyapatite nanoparticles, which were printed through micro-CLIP [74].

2.1.4. Liquid Crystal Display (LCD)

Further development from DLP has led to LCD-based stereolithography. In this method, the micro-mirror and lens set is replaced with an LCD screen powered by UV-emitting LEDs. These, like DLP, can irradiate or suppress each pixel; therefore, as the LEDs project the part's cross-section, the liquid crystal screen launches this projection through the UV-transparent window to the resin in the vat [75]. The LCD-SLA also allows the whole layer to be exposed at a single step and to cure simultaneously, building the part layer by layer (Figure 7). Employing LCD-SLA for shape memory 4D-printed polymeric resins has effectively proved the ability of this technique to print high-quality 4DP components [76,77].

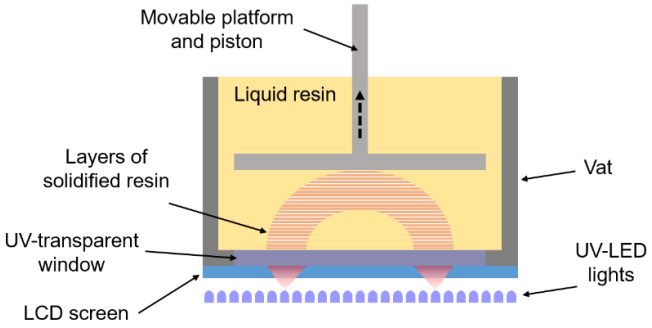

Figure 7. Schematic of a typical LCD printing method.

2.2. Material Jetting Techniques

In contrast to vat photopolymerisation 3D printers, material jetting technologies enable one to print different polymer materials in a single process, offering, for instance, the possibility to change colours, formulations or fabricate parts that have specific features localised at different positions [78,79]. In the case of photopolymers, material jetting relies on depositing droplets of liquid photoreactive resin on an *x-y* plane, which are immediately irradiated by a UV laser to initiate polymerisation at that spot and prevent material waste, by-products and debris [80–83]. These technologies evolved from single-layer 2D-printing techniques; hence, the three-dimensional part is built as ink deposited layer by layer [81,82,84]. The MJ printer jets at least two materials, i.e., build material and support material [85]. After printing, the jetted materials will be immersed in a solution to dissolve the support material. Some technologies, such as Stratasys' polyjet or 3D Systems' multijet printing, use an additional layer-levelling process before curing [86–88]. It should be noted that polyjet and multijet printing are trademarks representing MJ technology. The two common sorts of 3DP liquid-based jetting materials are CIJ 3D printing and DoD 3D printing.

2.2.1. Continuous Ink Jetting (CIJ)

CIJ comprises a printing head that ejects a photocurable ink onto a substrate as an accurate *x-y* coordinate system leads the droplets to be deposited at specific locations. The printing head has a UV-emitting source and one or more nozzles (Figure 8), each nozzle delivering a continuous jet of ink that readily splits into droplets and is subjected to UV-photoinitiated curing to coalesce once they reach the substrate [81,82,89]. This jet splitting would naturally be random, causing the droplets to have varying sizes; nevertheless, applying a piezoelectric transducer that generates periodic mechanical oscillations can correct

and control the stream [90]. As the droplets exit from the nozzle, they are electrostatically charged. The amount of charge is associated with the corresponding pixel on the image to be printed. Thus, an electric field is applied to deflect the droplet and guide it to a specific position where it should land on the x-y plane [90]. However, an issue challenging the effective use of CIJ for 3DP functional materials is the undesirable charge repulsion effects that arise as charged droplets become closer. Phung and Kwon (2022) proposed a novel voltage-driving scheme for selective area coating applications to overcome that issue [89]. In this sense, CIJ has promising potential for 4D-printed smart materials, including photopolymer-based composites reinforced with metallic nanoparticles and carbon nanotubes [80,91]

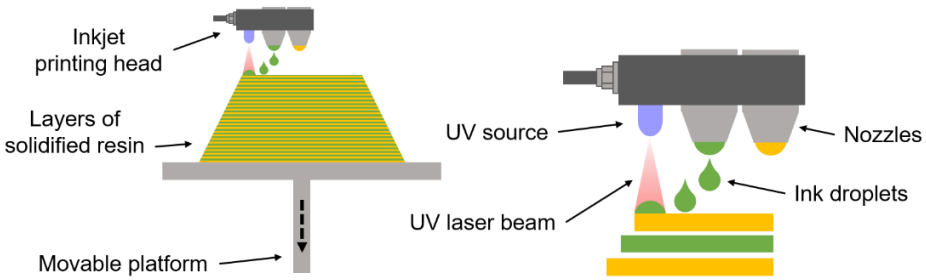

Figure 8. Schematic of a typical CIJ printing method.

2.2.2. Drop on Demand (DoD)

Material jetting has been further developed into DoD technology. It differs from CIJ as the ink flow is fully controlled and released only when needed, i.e., on demand, instead of continuous jetting [83,90–92]. The printing head nozzle contains a small reservoir or chamber where ink is stored while printing is not required, and two types of mechanisms can be employed to release an ink droplet, either piezoelectric or thermal (Figure 9). In the former, piezoelectric transducers deform as they receive an electric pulse, squeezing the chamber and launching a droplet [84,91,92]. In the latter, an electric pulse activates a thermal resistor that, within a timeframe in the order of microseconds, warms up the ink, producing an expanding bubble through rapid evaporation; hence, as the pressure in the chamber increases, the droplet is finally ejected from the nozzle [84,90,91]. The piezoelectric inkjet exhibits an essential advantage over the thermal one, as the temperature rise represents considerable risk and could dramatically affect the product properties [91].

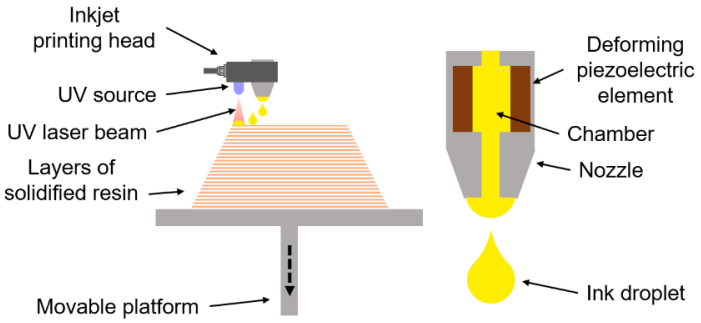

Figure 9. Schematic of a typical DOD printing method.

Moreover, DoD possesses a broader range of photoreactive inks with varying properties since the electric pulse can be optimised to meet each ink formulation requirement. In comparison, CIJ is limited by a narrower range of viscosity and surface tension [83]. DoD is suitable for processing materials that find applications in a number of different fields, including electronics, pharmaceuticals and, of course, rapid prototyping [83,93,94].

2.3. Material Extrusion Technique (Direct Ink Writing (DIW))

DIW is a 3DP technology similar to other extrusion-based AM techniques such as fused deposition modelling (FDM) (also called fused filament fabrication (FFF)), with a difference that in DIW, the printed material is not molten but rather it is semi-liquid or paste-like [95–101]. In addition, DIW also differs from other material jetting techniques as it delivers continued material (Figure 10) rather than splitting it into droplets, as in CIJ and DoD [100]. In DIW, the material is released from a nozzle as the result of applied pressure, which can be generated either mechanically (through a rotary screw) [98–100] or pneumatically (with a piston) [100,101]. DIW is claimed to be able to deliver efficiently and accurately 3D-printed micro-lattice structures, as well as to possess one of the broadest ranges of rapid prototyping ink designs, making a vast number of possibilities feasible in terms of shapes and styles [99,100].

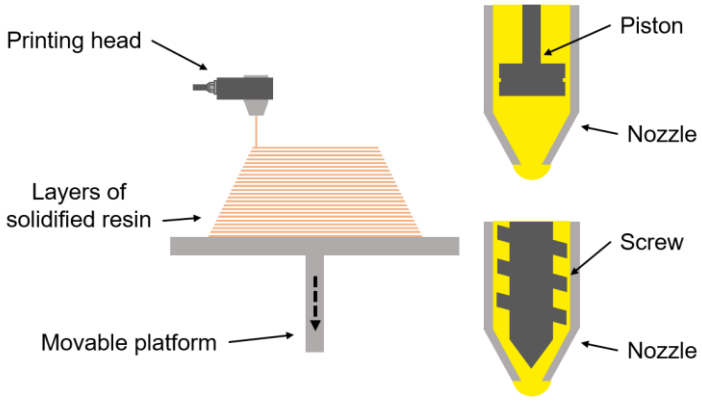

Figure 10. Schematic of a typical DIW printing method.

Materials for DIW inks are often formulated to solidify immediately or shortly after they exit the nozzle and, frequently, they are subjected to a photocuring stage so that they harden, which can be performed simultaneously with the printing process or after fabrication [97,100]. Furthermore, it is noteworthy that such inks typically present greater mechanical strength and can consist of highly viscous materials and fillers, such as organic or nonorganic particles, to impart shape retention after deposition [98,100]. According to Yang et al. (2021), DIW inks should present high viscoelasticity before extrusion, exhibiting an excellent shear-thinning effect when moving through the nozzle and recovering the viscoelasticity after deposition to retain the desired shape [98]. DIW faces challenges regarding the formulation of composite or functional inks that simultaneously possess the required shear thinning and modulus, as well as the ability to flow under shear stresses without issues and readily restore the previous viscoelasticity [100]. Notwithstanding such matters of concern, DIW finds applications in several fields and has successfully been used to 3D-print mixtures of ammonium oleate with polymers, such as natural rubber, PVDF and epoxy resins [98]; graphene-based paste for prototyping aerogels [99]; cellulose nanocrystal paste [101]; polycaprolactone-reduced graphene oxide composites [102]; PLGA composites reinforced with calcium phosphate and graphene [103]; and polymer-based hydrogels for biomimetic soft robots [104].

3. Mechanisms of 4DP and SMP

3.1. 4D Printing Mechanism

4DP can be defined as the 3DP of smart materials using a well-programmed design. In recent years, 4DP technology, with time as an extra dimension, has attracted substantial attention due to its flexibility in fabrication, cutting-edge results and promising future capabilities for different complex structures, with a preference for cost-efficient selection. In addition, this exceptional technology is considered challenging for traditional fabrication methods and valuable in solving various manufacturing issues by producing a variety

of metamaterial prototypes. It can be applied in wide temperature and humidity ranges. Therefore, combining 3DP technology with shape memory behaviour can provide smart devices with complex structures [105–107]. For example, the 4DP of grippers is produced using photocurable methacrylate-based resin via a micro-stereolithography printer and provides a good indication of the material's flexibility, controlling recovery and high strain of the gripper to grab objects, as shown in Figure 11 [55]. Alshebly et al. [108] programmed folding structures of a box produced so that the box folding can lock itself through a folding sequence for each section move. The boxes are fabricated using jet spraying and UV curing via a multijet 3D printer (Object Connex 260, Stratasys) with commercial epoxy/acrylate-based resin.

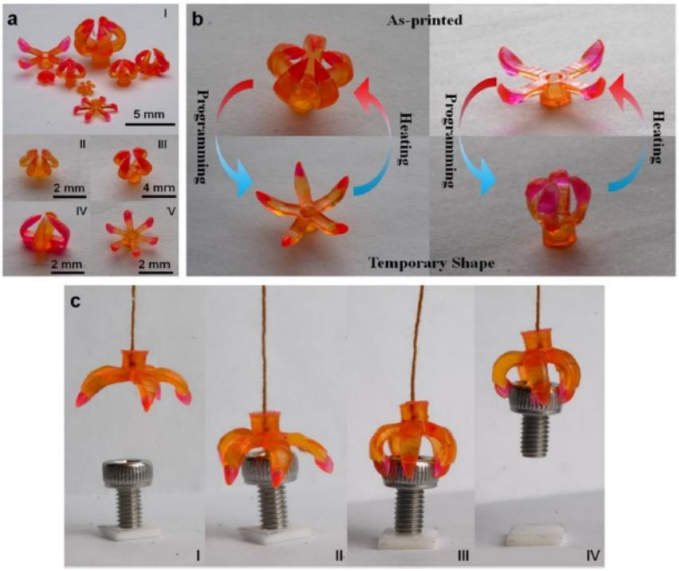

Figure 11. SLA-printed gripper with five arms. The gripper is small but with enough strain to hold a bolt [55]. (**a**) Multimaterial grippers are fabricated with different designs. (**b**) The explanation of the transition between as printed shape and temporary shape of multimaterial grippers. (**c**) The snapshots of the process of grabbing an object. Copyright © 2016, Scientific Reports.

3.2. Shape Memory Polymer Mechanism

There are two procedures for SMPs, temporary shape and permanent shape recovery. In the temporary shape process, physically, the entropy increases when the polymer is heated, which decreases the difference between entropy and an internal energy that leads to increased movement in polymer chain orientations and, thus, increases the polymer deformability. Consequently, the polymer can deform into a desired temporary shape upon applying an external force. The temporary shape can be fixed for a long time (shape fixity, Rf) by cooling and then removing the external force. Furthermore, the temporary shape can be controlled to maintain the desired shape, depending on the designed strain (ε_1) and the external force. This temporary shape with a strain of (ε_2) can be gradually reformed to the original permanent shape with a strain of (ε_3) without external force during reheating (shape recovery, Rr) (Figure 12). The shape fixity and shape recovery can be calculated from the equation below:

$$R_f = \frac{\varepsilon_2}{\varepsilon_1} \times 100\% \quad (1)$$

$$R_r = \frac{\epsilon_1 - \epsilon_3}{\varepsilon_1} \times 100\% \quad (2)$$

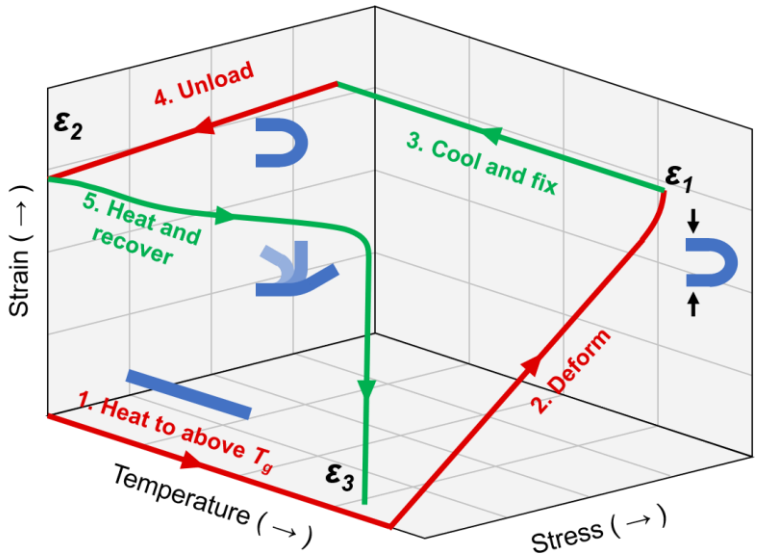

Figure 12. Shape memory behaviour and thermomechanical cycle.

Therefore, SMPs/SMPCs utilise a dual behaviour. The first is high elastic behaviour related to chemical crosslinking, molecular entanglement or the crystalline phase. The second behaviour is reversible in that the temporary shape can return to the original shape with a stimulus such as heating (Figure 13). This phenomenon is related to the glass transition temperature (T_{trans} or T_g) and reversible molecular crosslinking structure. The shape recovery occurs by releasing the stored strain energy in the temporary shape. Therefore, the fixed and reversible process represents the shape memory behaviour of the SMPs/SMPCs [43,109,110].

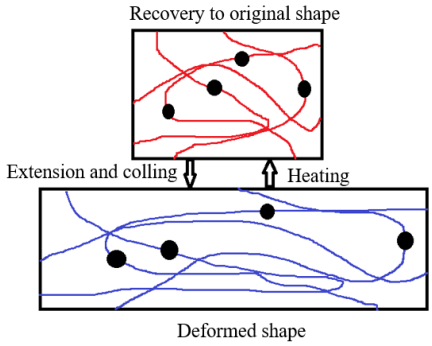

Figure 13. Shape memory thermally induced.

4. Materials for Liquid-Based 4DP and Shape Memory Nanocomposites

4.1. Materials for Photopolymerisation Techniques

Several materials can be included within the mixture resin of the photopolymerisation technique, such as photoinitiators, monomers/crosslinkers, inhibitors, diluent/solvent and fillers (particles and fibres). Inhibitors and retarders are additives essential for controlling the penetration depth and gelation time as well as limiting the adverse impacts of reflected photopolymerisation light [111]. Diluents/solvents are commonly used to decrease the resin viscosity, increasing the flow rate and enhancing recoating capabilities [112].

4.1.1. Photoinitiators

Photoinitiator molecules generate reactive species to link between the light source and the resin mixture to initiate photopolymerisation. Photoinitiators are in the form of solid or liquid that should be dissolved in the mixture resin. Generally, there are two types of reactions in photopolymerisation processes, radical and cationic (Figure 14) [113].

Initiation occurs under light irradiation, in which a photoinitiator or photoinitiator system is responsible for converting photolytic energy into the reactive species [114–116]. The photoinitiating systems for 3DP applications are discussed here, while the mechanisms of the photoinitiation reactions are comprehensively discussed in reviews [39,117,118]. Table 1 presents a list of radical and cationic photopolymerisation systems and their advantages for additive manufacturing.

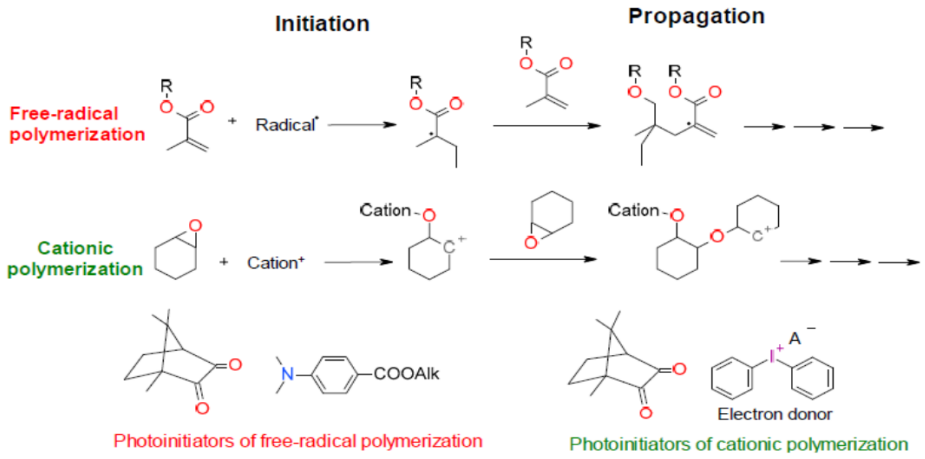

Figure 14. Mechanism of radical and cationic photopolymerisation [113].

A radical photoinitiator is commonly used to commence crosslink reactions in UV photopolymerisation for 3DP. It works perfectly with UV absorption wavelengths around 400 nm that are frequently used with SLA [49,119], DLP [120–124] and LCD [76] 4DP. Several researchers employed radical photoinitiators in the 4DP of shape memory polymers. Choong et al. [49,63,125] explored using phenylbis (2,4,6-trimethylbenzoyl) phosphine oxide (BAPO) (Table 1) as a photoinitiator, which was initiated under a wavelength of 405 nm for SLA and DLP 3D printers. BAPO (Irgacure 819) is commonly selected to match a projection/laser wavelength of 325 nm to 410 nm. It is more efficient in absorbing light to cleave and generate radicals to cure the mixture resins in 4DP [8,10,68,123,126–144]. The second widely used radical photoinitiator is Diphenyl (2,4,6-trimethylbenzoyl) phosphine oxide (TPO). Like BAPO, TPO is an alpha cleavage radical photoinitiator used with the same wavelength range as key processing to support the photopolymerisation process of 3DP [76,124,137,143–149]. Other commercial radical photoinitiators used to initiate photocuring are Ethyl (2,4,6-trimethylbenzoyl) phenyl phosphinate (TPO-L) [150–152], 1-hydroxycyclohexyl phenyl ketone (Irgacure 184) [51,153], 2,2-dimethoxy-2-methylpropiophenone (Irgacure 651) [154], bis(2,6-difluoro-3-(1-hydropyrrol-1-yl)phenyl) titanocene (Irgacure 784) [155] and 2-hydroxy-2-methylpropiophenone (Irgacure 1173) [156]. The disadvantages of radical photopolymerisation are the high shrinkage during curing and the oxygen inhibition. Oxygen inhibition, in most cases, is considered to be an undesirable property due to preventing photopolymerisation in thin films and creating tacky surface layers for thick films, which can affect the shape stability of 3D-printed components [50,157,158].

Compared to free radicals, cationic photoinitiators are insensitive to oxygen and better used within thermocurable resins, such as epoxies or vinyl ethers, to obtain good mechanical properties and less shrinkage, despite the disadvantage of a slow curing rate [159]. Thermocurable resins are thermally stable and need high energy to cure. Therefore, due to their solubility and thermal stability, cationic photoinitiators such as Onium salts (sulfonium) have excellent light absorption at high wavelengths over 300 nm [39]. Cyracure (UVI-6976) is a cationic photoinitiator containing a mixture of triarylsulfonium hexafluoroantimonate salts in propylene carbonate. UVI-6976 is most effective in a range of 210 nm to 350 nm, used by several researchers as a cationic photoinitiator for curing epoxy and

epoxy/acrylic mixture resins [160–163]. Yang et al. [164] employed UVI-6976 to initiate fast UV curing for epoxy-based mixture resin under UV source and ink-jet printing.

Furthermore, radical and cationic photoinitiators can produce a hybrid radical cation effect by reacting to various photopolymerised liquids, such as epoxy/acrylate-based mixture resins [46,50,165,166] (Table 1). For instance, Kuang et al. [123] employed Epikure 3253 (2,4,6-tris-dimethylaminomethyl phenol), Sudan and BAPO as initiators with a ratio of 0.1 wt%:0.07 and wt%:0.4 wt%, respectively, under a DLP wavelength of 385 nm for epoxy/methacrylate-based mixture resins. Al Mousawi et al. [166] used a blend of photoinitiators, namely Zinc Tetraphenylporphyrin (ZnTPP) and Bis(4-tert-butylphenyl) iodonium hexafluorophosphate (Iod). The ZnTPP/Iod salt is used as a UV-sensitive compound with a ratio of 0.5 wt%:1 wt%, respectively, which results in high photocuring ability for epoxy/acrylic resin systems via a UV light source, with a wavelength range of 375 nm to 550 nm. Diphenyliodonium hexafluorophosphate (Iod) and 9-Vinylcarbazole (NVK) are used with BAPO under a UV source with a wavelength greater than 290 nm to enhance the curing rate of the hybrid epoxy/acrylate resin [167,168]. (NVK/Iod) initiator system with a ratio of (3 wt%/2 wt%) is included for acrylate radical and epoxy ring opening as a high-performance photoinitiator.

Table 1. List of radical and cationic photopolymerisation systems and their advantages for additive manufacturing.

Photoinitiator	Method	Wavelength	Composition	Nanofiller	Content	Advantages
Irgacure 819 (BAPO)	DLP & SLA	405 nm	Acrylate-based (tBA, DEGDA)	SiO_2	0, 1, 2.5, 5 and 10 wt%	High shape fixity, shape recovery and cycling stability. Improved build speed, surface quality, tensile strength and break strain [63,125].
Irgacure 819 (Bapo)	DLP		Epoxy/acrylate-based (EA, IBOA, and HDDA)	Au	0.01, 0.025, 0.05, and 0.1 wt%	Programmable light-activated 4DP SMPCs with tuneable transition temperatures that can be activated by light are useful for remotely controlling morphing, especially for the actuator and soft robotic applications [169].
Irgacure 819 (BAPO) and Sudan	DLP	405 nm	Epoxy/acrylate-based (2PA, IBOA and TMPEOTA)	ZnO	0, 1, 2.5, and 5 wt%	Enhance curing speed, surface quality, tensile strength, fracture strain and elastic modulus [122].
Irgacure 819 (BAPO)	DLP	385 nm	Acrylate-based (PHEMA and PEGDA)	CNT	0.1, 0.3, and 0.5 wt%	High shape fixity (Rf) and shape recovery (Rr) ratios achieved (Rf ≈ 100%, Rr > 95%) confirmed the significant electrically triggered responsiveness of such CNT/SMPCs [139].
Irgacure 819 (BAPO)	UV source & DIW	-	Epoxy/acrylate based (DGEBA, BA, Ebecryl 8402 and Tris)	TiO_2		Improve tensile toughness and shape memory properties [170].
Irgacure 819 (BAPO) and NVK & Iod (DPIHFP)	UV source	>290 nm	Epoxy-based (ECC, Tris and hydrochloric acid	MWCNT	0.5 and 1 wt%	Improve the mechanical strength and filler dispersibility. MWCNT has a dual role as a co-initiator that enhances the polymerisation speed. However, the reactivity drops drastically at high loadings of MWCNTs due to blocking the UV light [167,168].
-	DLP	-	Acrylic-based, commercial-DLP ink (Are3d-dlp405)	MWCNT	0.1, 0.2, 0.3, 0.4, 0.5 and 0.6 wt%	Enhance shape memory properties, electrical and thermal conductivity [64].
Irgacure 819 (BAPO), Epikure 3253 and Sudan	DLP	385 nm	Epoxy/methacrylate-based (Epon resin 828, ETPTA and 4-MHHPA)	-		Increase printing speed with high resolution, low volume shrinkage and excellent mechanical properties [123].
TPO	DLP	405 nm	Acrylate-based (tBA and HDDA)	-		Improve shape fixity, shape recovery and excellent cycling stability with good thermal stability [124].
TPO	LCD	405 nm	Epoxy acrylate (EA) and (IBOA, TMPTA)	-		High shape recovery rate and excellent cycling stability. In addition, prospect application as a smart electrical valve actuator [76].

Table 1. *Cont.*

Photoinitiator	Method	Wavelength	Composition	Nanofiller	Content	Advantages
TPO-L	UV source	300 nm to 450 nm	Epoxy/acrylate-based (DGEBA, Diuron™, DICY, SR349 and micro-carbon fibres)	SiO_2	7 wt%	Enhance thermo-mechanical properties and fast UV curing [159].
Cyracure (UVI-6976)	UV source and inkjet	350 nm	Epoxy/acrylate-based (DGEBA, PEG, EGDGE and NGDGE and BGDGE and BF3 and triethylamine)	-		Low-cost, material-saving, environment-friendly and fast manufacturing with using UVI-6976 [164].
Omnirad 184, and IPF	SLA	355 nm	Epoxy/acrylate-based (DGEBA, DGEHBA, OXT, DGEDA, TMPTA-EO3 and DSM)	-		Good shape fixity, shape recovery and excellent cycling stability. In addition, high thermal stability, strength, break strain and toughness [50].
ZnTPP, IPF and Esacure 1187	UV source	375 nm to 550 nm	Epoxy/acrylate-based (PBN, TEGDMA and EPOX)	-		High-performance photosensitive resin for LED projector and LCD screen [166].
1-Hydroxycyclohexyl phenyl ketone and GLYMO	SLA	355 nm	Epoxy/acrylate-based (DGEBA and BA)	SiO_2	8 wt%	Improve tensile strength, tensile modulus, flexural strength and heat stability [171].

4.1.2. Polymers for Photopolymerisation

Selecting a liquid monomer/oligomer suitable for 4DP via the photopolymerisation technique is connected with choosing parameters and materials, such as light wavelength, curing speed, layer thickness, photoinitiator, crosslinker and fillers (particle and fibre). This optimization is carried out to obtain the desired properties for the printed components, such as good shape memory, dimensional accuracy and mechanical properties. In addition, the monomer/oligomer tends to be polymerised with a radical, cationic or hybrid photopolymerisation process. For example, acrylate and methacrylate monomers are widely used in radical photopolymerisation due to fast photocuring in spite of geometric stability and high shrinkage during curing. On the other hand, epoxy and vinyl monomers used in cationic photopolymerisation have good thermal and mechanical properties in addition to less shrinkage. Therefore, several studies employed hybrid epoxy and acrylate resins to obtain favourable characteristics. However, the thermally cured epoxide resins still did not spread in 4DP like acrylic resins because ionic polymerisation takes longer in terms of curing time [172–174].

The (meth)acrylate-based resins are used in 4DP due to the molecule structure flexibility that can be included with various radical photoinitiators, crosslinkers and other additives under fast photopolymerisation curing rates. For instance, many researchers used Tert-Butyl acrylate (tBA), due to shape memory ability, with a crosslinker, such as poly(ethylene glycol) Di-methacrylate (PEGDMA) [175], 1,6-hexanediol diacrylate (HDDA) [124] and Di(ethylene glycol) diacrylate (DEGDA) [49,63,125]. Moreover, poly hydroxyethyl methacrylate (PHEMA) [139] and Bisphenol A-glycidyl methacrylate (BisGMA) [166] have also been employed to demonstrate good shape memory properties.

On the other hand, the most epoxied polymer used in 4DP under cationic polymerisation is Bisphenol A diglycidyl ether (DGEBA) [159,164,170] (Table 1) due to showing excellent shape memory and mechanical properties. DGEBA is mixed with a suitable cationic photoinitiator and additives to improve the curing rate, as mentioned in the previous section. Epoxy-based resins require a longer time to cure after photopolymerisation, which can enhance the strength of the 4D-printed component [67]. Radchenko et al. [176] explored using a cycloaliphatic epoxy-based resin with a cationic initiator diaryliodonium hexafluoroantimonate (DPIHFP) as a candidate mixture resin for SLA 4DP to enhance the mechanical and shape memory properties.

Recently, the research area about hybrid mixture photopolymerizable resins using dual-stage curing has been expanded due to improving several mechanical, thermal and shape memory properties. The hybrid resin is commonly composed of photocurable resin and thermal curable resin, such as acrylates and epoxides, respectively, that results in a high curing rate, low shrinkage and insensitivity to oxygen. Furthermore, many researchers have revealed that cationic polymerization has been fostered by using radical photoinitiators, in which an interpenetrating polymer network (IPN) structure is established upon the multi-curing mechanism. The hybrid resin is cured by UV light during 3DP and then using thermal cure to yield IPN epoxy composites [159,177]. For example, high shape fixity, shape recovery and thermomechanical cycling stability, in addition to good strength, toughness, thermal stability and failure strain, can be obtained by using hybrid resins such as Bisphenol A diglycidyl ether (DGEBA) with ethylene oxide-modified trimethylol propane triacrylate (TMPTA-EO3) [50] (Table 1). Schwartz and Boydston [161] blended epoxy/acrylate-based resin systems with corresponding BAPO as a radical initiator and triaryl sulfonium salts as a cationic initiator to produce multifunctional components with improved mechanical anisotropy and spatially controlled swelling that facilitates 4DP.

4.2. Materials for Material Jetting Technique

Like no other 3DP technology, the material jetting (MJ) technique uses multicolour and multimaterial resins due to the use of multiple nozzles per print head, which can be employed to print SMP and hydrogel multimaterial. It is most challenging to manufacture functional components by including nanoparticles via the MJ technique due to

rheological requirements for the resin, such as low viscosity, despite the printer heating the resin to obtain an appropriate viscosity [178]. The MJ 3DP commonly uses polyethene-based (PET) and polyethylene-based (PEN) resins to fabricate wearable electronic parts [179]. Biomedical scaffolds and cells are usually printed via the MJ 4DP using smart polymers [180,181].

Many materials are used for MJ techniques, such as casting wax, thermoplastic, thermosetting and elastomeric. Most MJ 3D printers work only with their commercial materials and do not have an open mode. The commonly used commercial resins are Fullcure, VeroBlue, VeroBlack [182], MED610 and RGD 525 [30] due to high accuracy and good mechanical and thermal properties. On the other hand, the multiple nozzles allow for the dispensing of various materials with multicolour throughout a single print. Moreover, the MJ process is fast and provides extreme accuracy and soluble support for the prints. However, MJ 3D printers and their materials have high cost because of these advantages [20]. For example, as reported in the literature [183–185], the blue fibres (Verocyan) and yellow fibres (Veroyellow) can be used as digital SMPs, whereas the sky-blue matrix (Tango+) is a rubber-like transparent material. Jeong et al. developed a multicolour structure using the polyjet process. They achieved controlled shape changes by manipulating the colour of light and the illumination timing. In addition, these SMPs can be reused by reprogramming thermodynamically, and their response temperature can be adjusted by dynamic mixing during material synthesis or 3DP.

Cheng and Huang reported a strategy of preparing light-curing resins to develop full-colour 3D-printed components via a bespoke MJ printer. They investigated the effects of various concentrations of TPO photoinitiator for different kinds of crosslinkers and polymers (acrylate, polyurethane and polyester) on the curing rate and degree of swelling. They found that the components of 70 wt% Isobornyl Acrylate (IBOA), 20 wt% aliphatic polyurethane acrylate (PUA), 10 wt% Tripropylene glycol diacrylate (TPGDA) and 3% Diphenyl-(2,4,6-trimethylbenzoyl)-phosphine oxide (TPO) exhibited a reasonable curing rate, low volumetric shrinkage and good dimensional accuracy [186].

Ding et al. [187] explored a direct 4DP approach to investigate the SME using a polyjet technique that jets multimaterial ink droplets in a layer and cures them with ultraviolet light. They employed several commercial materials, such as TangoBlack+ or Tango+, as the elastomer and VeroClear as the SMP. Upon heating, the SMP softens and permits the object to change into a new permanent shape, which can then be reprogrammed into multiple consequent forms. In addition, it integrates five separate printing and programming steps (Figure 15a) into one single step. The 3D-printed component can rapidly change its shape upon heating (Figure 15b).

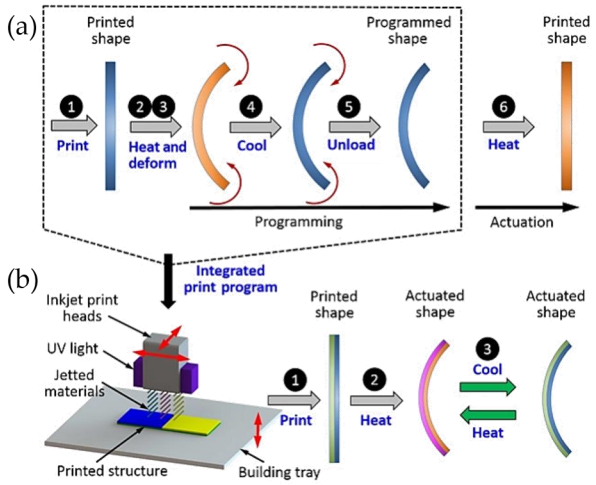

Figure 15. Demonstration of polyjet 4DP, (**a**) previous SMP-based 4DP requests five steps to achieve the programmed shape. (**b**) The direct 4DP approach allows for fabricating controlled multimaterial composites to integrate the five steps into a single one [187]. Copyright © 2017, Science.

4.3. Materials for Direct Ink Writing Extrusion Technique

As previously stated, the choice of resin polymer for liquid-based 3DP depends mainly on the method of curing this resin during production. As a material extrusion technique, direct ink writing recently gained much attention due to employing a variety of monomers/oligomers, thickeners, nanoparticles and micro/nano-fibres materials using a processing condition with minimal residual stresses [188]. The most crucial issue facing DIW 3DP is modifying ink's rheology to be a printable thixotropic fluid, and this modification can be achieved by incorporating additives such as nanoparticles. A list of DIW 4D-printed shape memory nanocomposites and their improved properties is presented in Table 2. In addition, DIW requires the material itself to be shear thinned for extrusion through a fine nozzle and maintain its shape after extrusion. For thermally cured resins such as epoxy-based mixture resins, most DIW 3DP uses a multi-cure or dual-cure approach system that applies UV-cure and/or thermal-cure UV during or after extrusion using an oven with temperature ranges of 100–185 °C [11].

Table 2. List of DIW 4D-printed shape memory nanocomposites and their improved properties.

Nanoparticle	Content	Base Resin	Method	Improvement
Nanosilica	8 and 10 wt%	Epoxy and short carbon fibre	DIW	Good shape retention, shape recovery and high storage modulus [189].
Nanosilica	7, 10 and 13 wt%	Epoxy/polybutadiene rubber	DIW (Hyrel 3D hydra 16), then thermal curing	Improved toughness, strain at break, shape recovery and thermomechanical cycle [11].
Nanoclay	12.0, 13.5, 15.0, 16.5 and 18.0 wt%	Hydrogel mixture with TPO as UV initiator	Homemade DIW, then 425 nm UV source	Smart hydrogels and shape-changing memory polymers [145].
Nanoclay	25 wt%	Polyimide/methacrylate	DIW with UV- assist	Improve shape fixity, shape recovery and mechanical properties [190].
Graphene nanoplatelet	5.0, 7.5, 10.0, and 12.5 wt%	Commercial bisphenol epoxy	DIW	Increasing thermal and electrical conductivity and improving thermo-induced shape memory performance [191].
Graphene nanoplatelet	0.1, 0.2, and 0.3 wt%	Epoxy-based SMP	DIW with cryo-system-assisted	Shape recovery, storage modulus, loss tangent, tensile strength and elastic modulus are increased [192].
Barium titanate	0, 10, 20 and 30 wt%	Polylactic acid (PLA)-based and short carbon fibre	DIW	Good shape memory and sensing capabilities, with the robust sensor capable of withstanding temperatures ranging from 23 °C to 100 °C [193].

Wan et al. [194] summarised, in their review, materials that have enabled 4DP through DIW in recent years. Among various SMPs/SMPCs, epoxy-based composites are known for their high modulus and strength. To realize the solid-like state of epoxy, Compton et al. [195] used nanoclay, while Lewicki et al. [196] used fumed silica to modify epoxy to meet the rheological requirements. Guo et al. utilised an industrial-grade epoxy, di-glycidyl ether of bisphenol-A mixed with curing agent methylhexahydrophthalic anhydride (MHHPA), 1.0 wt% accelerator benzyldimethylamine (BDMA) and 10 wt% fumed silica. The prepared printable ink showed good shape retention with excellent mechanical performances below and above the T_g of epoxy. In addition, the composite components' shape fixity and recovery ratios reached 100% and more than 96%, respectively [189]. Furthermore, a series of thermoset shape memory composites can also be used with DIW 3DP. For instance,

Rodriguez et al. [197] chose environmentally friendly and renewable epoxidised soybean oil (EBSO) as the matrix. The bisphenol F diglycidyl ether (BFDGE) was added to the matrix to increase the mechanical strength and optimise the mass ratio. The addition of carbon nanofibres (CNFs) tailored the rheological properties of the ink to obtain shear-thinning performance and endowed the printed structures with an electrical response. With the help of origami, a complex box-like shape was obtained by folding the grid pattern and cured completely. Then, it was unfolded into a temporary shape. Upon reheating above T_g, the box recovered to its folded shape [197]. In addition to the thermoset SMPs, thermoplastic SMPs, such as polylactic acid (PLA)-based inks [198], poly (D,I-lactide-co-trimethylene carbonate) (PLMC) [199], polyurethane and polyethylene oxide (PEO) [200], have demonstrated actuated behaviours after DIW printing. Wang et al. synthesised waterborne shape memory polyurethane (SMPU) mixed with polyethylene oxide (PEO) or gelatin in water to enhance the viscosity of the ink. The PEO exhibited better shape memory properties, while gelatin exhibited better biocompatibility. They found that adding superparamagnetic iron oxide nanoparticles (SPIO NPs) promoted osteogenic induction and shape fixity. The printed scaffolds showed faster and better shape recovery properties in water than in an oven [200].

Several studies have used DIW 3DP to create 4D-printed structures of liquid crystal elastomers (LCEs) and silicone elastomers (SEs) [201–208]. Yamagishi et al. [201] manufactured thin-film-based liquid metals (LMs) injected with a microfluidic channel antenna with high deformability via DIW. In this study, a coil-shaped silicone sealant microfluidic channel was fabricated on a flexible/stretchable Ecoflex substrate, which was followed by the injection of gallium-based liquid metal in the microfluidic channel. The produced wireless light-emitting device worked via a standard near-field-communication (NFC) system and kept the same behaviour under deformations, including a uniaxial strain of around 200%, twisting of 180° and bending with a radius curvature of 3 mm. Long et al. [209] proposed controllable stiffness composites consisting of LMs as functional materials and SE as the encapsulation layer, respectively, using DIW 3DP. The authors selected three types of SE, including Ecoflex00-30, PDMS Sylgard 184 and SE 1700. In addition, various mixing ratios of silicone were adjusted to satisfy the required rheological condition for DIW. The results showed that at a high temperature, the resistance of the conductive composites changes with the deformation degree, which is expected to be applied in the field of soft sensing actuators.

Furthermore, LCEs are recognized by their reversible and anisotropic shape changes in response to an external stimulus because of their lightly crosslinked polymer networks [203]. Applying the DIW technique to the fabrication of LCEs is significant for producing LCEs with programmable stimuli-responsive behaviours and desirable 3D geometry in practice [210,211]. Almost all the potential applications of 4D printing developed on DIW using LCEs are actuators [203–208]. Extensive papers introduced and reviewed the usefulness of actuation behaviour, which can be activated by different stimuli, such as heat, light, humidity and electrical energy. Apart from actuators, soft robotics, LCE dissipators [212] and LCE optical devices [213,214] were also exploited via DIW. Compared to nonprinted thin-film LCE actuators, millimetre-thick LCE actuators realized by DIW printing can bring more excellent actuation capability required for artificial muscle or soft-body robot designs. Lopez et al. proved that the thermally driven behaviour of 4D-printed LCE tapes could lead to rotation of the central linear polarizer, showing potential applications in polarization monitoring or thermally guided optical transmission devices. By embedding thicker 4D-printed LCE rings in polydimethylsiloxane (PDMS) plates, they further demonstrated the possibility of 4D-printed LCE/PDMS combinations as focal lenses that vary with temperature [215].

4.4. Nanoparticle-Modified Printable Liquid-Based Resin

Nanocomposite polymeric resins offer opportunities to enhance several characteristics of 3D-printed components, such as shape memory, thermal, mechanical, electrical, curing

and shape accuracy. One of the shortcomings of polymer nanocomposites is the elongation at break, which may reduce with increasing the content of nanoparticles [216–219]. Several parameters should be controlled when using nanomaterials. For example, resin viscosity at a high loading level becomes difficult to mix, leading to increased curing time. Resin homogeneity is another challenge; hence, the chemical compatibility of the nanoparticle with the polymeric resin must be considered. In addition, poor interfacial adhesion due to nanoparticle aggregations acts as a stress concentration defect. Therefore, several researchers have applied surface modifications for nanoparticles, such as covalent or noncovalent functionalization, to enhance nanoparticle dispersion and decrease agglomeration [220–222]. In addition, leading-edge equipment is used for the mixing process, such as an ultrasonicator, vacuum centrifugal mixer, three-roll milling and three-ball milling, to enhance nanoparticle adhesion, dispersion and rheology of the polymeric resin. Therefore, chemical modification in the molecular chain and the inclusion of functional additives can improve printability. Thus, the 3D-printed components can be multifunctional in different applications [223–225]. The following sections will focus on various nanoparticles employed in 4DP. The common nanoparticles included within 4D-printed resins, such as nanosilica, nanoclay, CNT and nanographene, with their features are described in the following sections.

4.4.1. Nanosilica-Modified Polymeric Resin

Researchers have recently focused on using nanosilica due to its unique characteristics, such as high surface area, pore volume and scalable synthetic availability [220]. Nanosilica is extensively considered as a photoinitiator material in addition to enhancing shape memory and mechanical properties. Choong et al. [63] studied the effect of the inclusion of nanosilica up to 15 wt% on the shape memory and mechanical characteristics of the tBA-co-DEGDA mixture resin and photoinitiator BAPO using DLP. They found that nano SiO_2 forms multifunctional crosslinking that enhanced the tensile strength by 3.6-times more than pure resin, shape fixity by 100%, shape recovery by 97% and doubled the shape memory life cycle. Hence, the optimum results are obtained at a SiO_2 ratio of 2.5 wt%. Figure 16 shows that the curing curve of the nanosilica components achieves higher curing depths in a short time compared with the unfiled component. For example, the inclusion of 1 wt% nanosilica achieved a 54.2 µm curing layer in just 0.7 s, while the unfilled SMP achieved 12.5 µm after a curing time of 4 s. Hence, nanosilica is considered as a heterogeneous nucleation spot within the photopolymerised resin and, thus, can reach a high curing rate during the polymerization process (Figure 17).

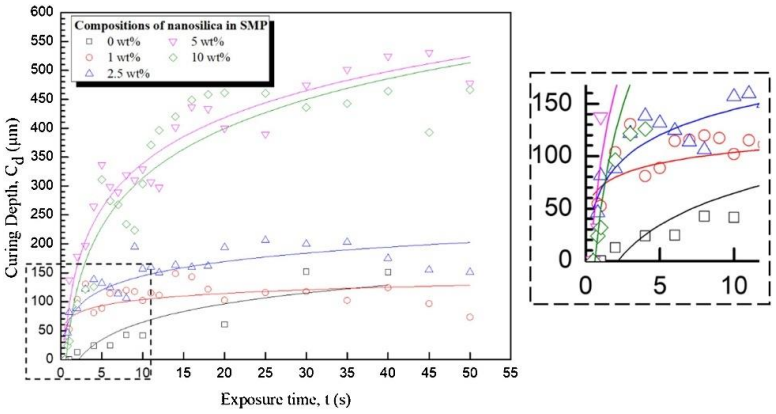

Figure 16. Curing depth versus exposure time of nanosilica/acrylic-based resin [63]. Copyright © 2022 Elsevier.

Griffini et al. [159] incorporated fumed silica within an epoxy–acrylate/TPO-L mixture resin with particle loading of 7 wt% as a thixotropic additive to enhance the photopolymerisation process of 3DP. Other research presented improvements in the curing rate, shaping accuracy, thermal and mechanical characteristics of photopolymerisation resins [226–231].

Gurr et al. [228] prepared novel optically transparent acrylic/nanosilica composites using SLA 3DP, and they noticed that the strength and dimensional accuracy were significantly enhanced. The high level of nanosilica that can be used without a decrease in curing light transmittance is 17 wt%.

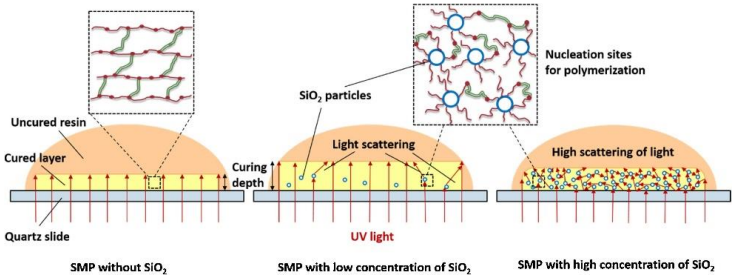

Figure 17. Schematic diagram of nanosilica acting as nucleation spots to initiate polymerization [63]. Copyright © 2022 Elsevier.

Numerous polymeric resins have good shape memory and mechanical properties when printed by DIW printers. However, these resins may lack printability (low viscosity and slow curing rate). Therefore, some functional additives are included, such as nanoparticles, to thicken the matrix and enhance the printability process. For example, fumed silica is incorporated with silicone elastomers to modify printability, improve mechanical properties and duplicate the stretch [232]. Notably, nanoparticles can balance mechanical characteristics and shape retention ability. Nanosilica shows an excellent strengthening effect up to a weight content of 10 wt% [233]. In addition, nanosilica can enhance the interfacial adhesion between epoxy and carbon fibres [189,234,235]. Guo et al. [189] concluded that the rheology and printability of the epoxy-based resin for DIW 4DP are improved and lead to good shape retention, shape memory and excellent mechanical characteristics below and above the T_g with the inclusion of nanosilica, with a loading of 10 wt%. As demonstrated in Figure 18 for the sketches and optical pictures of 4D-printed epoxy resin filled with nanosilica of 8 wt% and 10 wt%, the component of 8 wt% nanosilica yields a much larger deviation, while the component of 10 wt% nanosilica displays good shape retention. In addition, the storage modulus (G′) is greater than the loss modulus achieved with nanosilica loading of 10 wt% (Figure 19). Hence, the high shear stress increased the fluidity of the mixture resin, which is considered the preferred property to facilitate extrusion through the nozzle. The same procedure of using nanosilica to modify the rheology of the resin and enhance printability was conducted by Chen et al. [11]. The authors employed a static mixing printhead and single extrusion printhead for DIW 3DP (Hyrel 3D hydra 163) to control the curing speed of the epoxy/polybutadiene rubber resin, with the effect of incorporating nanosilica of 7, 10 and 13 wt% (Table 2). The process followed by thermal curing involves first curing at 50 °C overnight (12 h), followed by 100 °C curing for 8 h and then 150 °C curing for 1 h. The improved properties were toughness by 135%, strain at break by 200% and shape memory recovery ratio by 94% within about 50 s after 10 thermomechanical cycles.

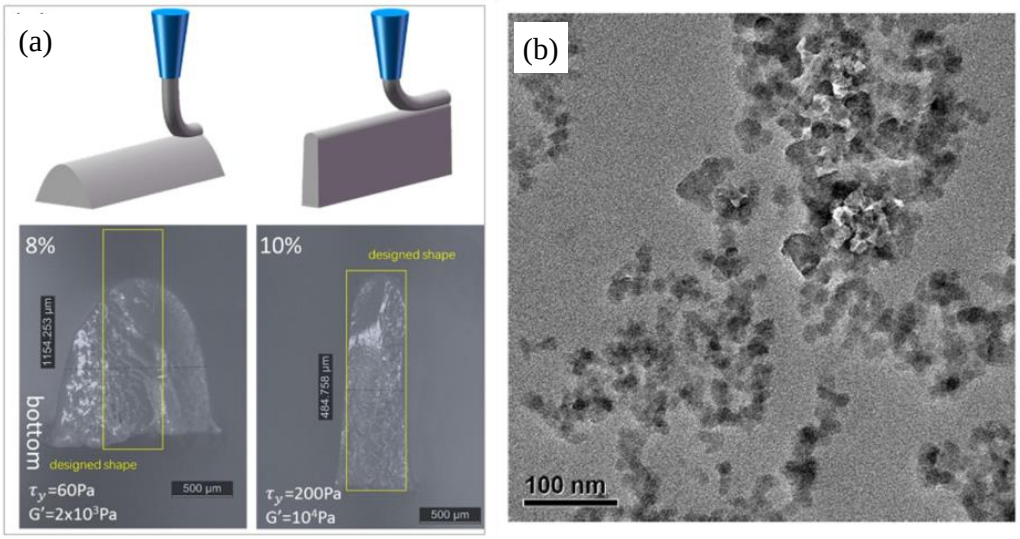

Figure 18. (**a**) Sketches and optical images of 4D-printed epoxy resin filled with 8 wt% and 10 wt% nanosilica, (**b**) transmission electron microscope micrograph shows nanosilica dispersion [189]. Copyright © 2022 Elsevier.

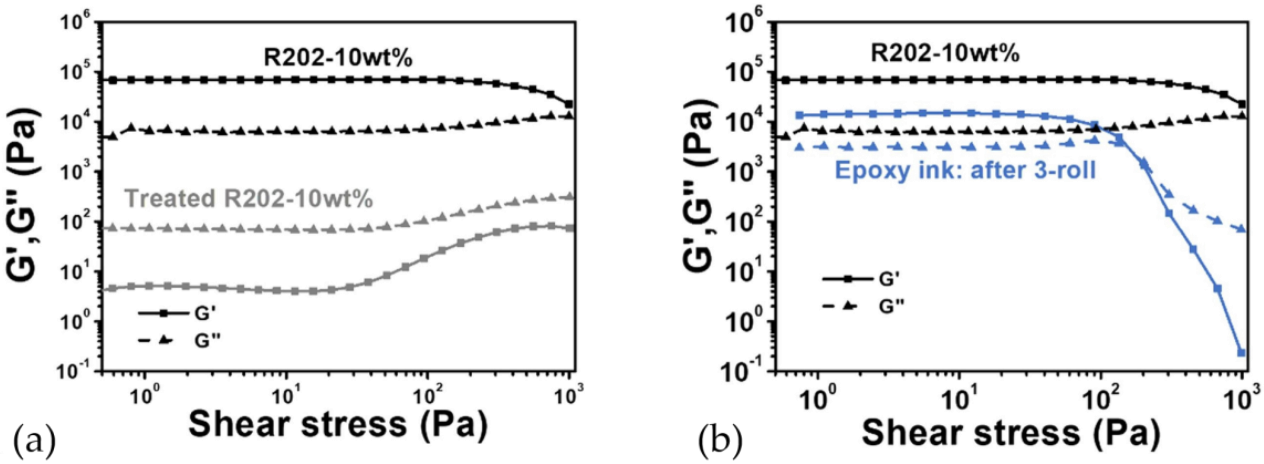

Figure 19. Storage modulus and loss modulus over shear stress of (**a**) 10 wt% nanosilica/epoxy component and nanosilica treated under high temperature, (**b**) before and after 3-roll milling [189]. Copyright © 2022 Elsevier.

4.4.2. Nanoclay-Modified Polymeric Resin

Nanoscale layered silicates (nanoclay) have attracted researchers within 3DP resin to improve strength, stiffness, toughness, flame retardancy and shape memory properties due to their high surface/volume ratio and platelet morphology, which produce good interfacial adhesion and enable free platelet orientation within the polymeric matrix [236–239]. Eng et al. [236] discussed the dispersion, alignment, size and content ratio of the nanoclay-modified commercial acrylate-based monomer via stereolithography. One dimension of the montmorillonite nanoclay is on the nanoscale, while the other two dimensions can be up to one micrometre that can be obtained at a high aspect ratio when exfoliation occurs into individual layers, resulting in increased surface bonding between the clays and the polymer matrix. Nadim et al. [237] investigated using nanoclay and fumed silica-filled epoxy ink with loadings up to 12.5 wt% and 10 wt%, respectively, via DIW. They noticed that the components' rheology, printability, strength and T_g were improved.

Li et al. [145] succeeded in 4DP a bilayer structure hydrogel mixture filled with nanoclay using homemade DIW. The authors improved the double hydrogel's swelling rate

and pores, which offered internal power for the rapid bending deformation. In addition, the two layers showed different swelling characteristics with increasing ambient temperature (Figure 20). The printed components were exposed to a 425 nm UV source to enhance the curing and finalization. Several other studies used smart hydrogels and shape-changing memory polymers as materials for 4DP [240,241].

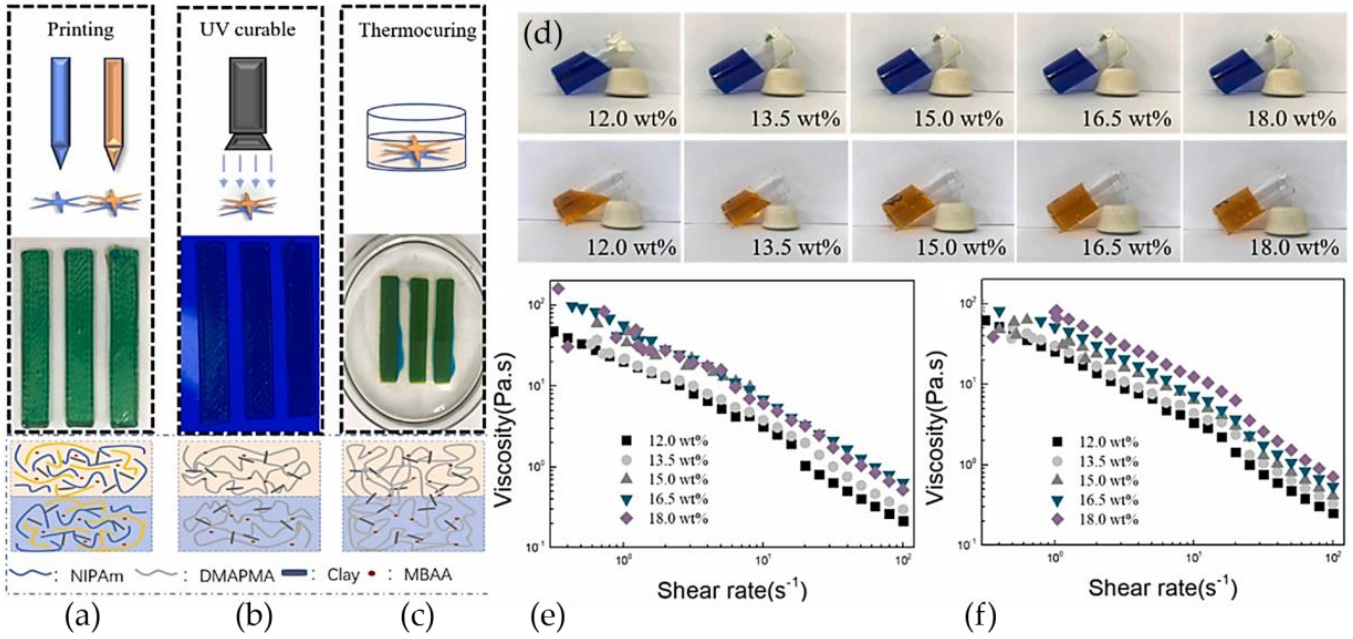

Figure 20. (**a**) Print process and print result photos, (**b**) photo of photocuring state, (**c**) thermo-curing process, (**d**) tilted photos of the two printing fluids with different clay content, (**e**,**f**) viscosity shear rate of top layer and bottom layer [145].

Another strategy was employed to manufacture lightweight nanocomposites that have a good shape memory effect (SME) by including clay nanoparticles, conducted by Li et al. [190], to develop polyimide/methacrylate resin for UV-assisted DIW 4DP (Figure 21). Nanoclay content of 25 wt% was added to SMPI for DIW 4DP to enhance the resin's shear thinning and storage modulus. The mixture resin is cured quickly under UV-induced free radical polymerization. The author also used DLP printing for the photoresin; the shape fixity and shape recovery are improved by 99.8% and 98.3%, respectively, while T_g is found to be 160 °C. Furthermore, the shape memory polyimide (SMPI)-based components were also improved with DIW extrusion moulding that can recover to their original shape in a few minutes. In addition, they characterised design diversity and space shape memory with 4DP of the self-folding box and stimuli-response gripper.

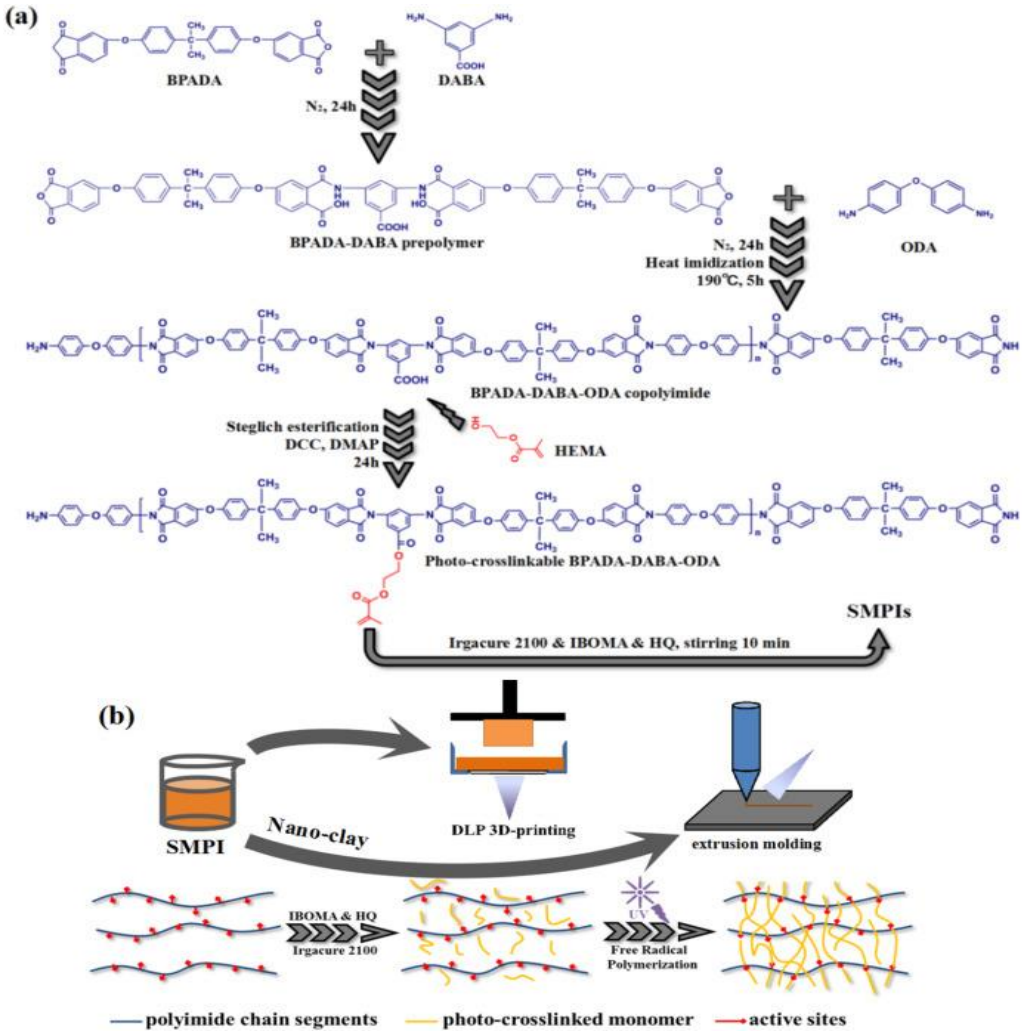

Figure 21. (**a**) A scheme of SMPI network preparation. (**b**) A schematic diagram of 3DP and extrusion moulding process [190]. Copyright © 2022 Elsevier.

4.4.3. CNT-Modified Polymeric Resin

Many researchers have used carbon nanotubes (CNTs) to modify polymeric matrices to improve several composite properties. Carbon nanotubes can be defined as cylindrical-shaped nanomaterial that is manufactured from graphite sheets. CNTs can be divided according to the number of carbon layers into three types: single-walled carbon nanotubes (SWCNTs), double-walled carbon nanotubes (DWCNTs) and multi-walled carbon nanotubes (MWCNTs) [242]. Appropriate dispersion and a high interfacial adhesion force between the CNTs and polymeric matrix are essential to include CNTs as effective reinforcement for polymer nanocomposites [243].

Zhang et al. [244] explored the influence of CNTs with loadings of 0.5 wt% to 2.0 wt% on the printability and electromagnetic wave absorption of acrylic ester nanocomposites using an SLA 3D printer. They found that up to 1.6 wt% CNTs have high printability under photopolymerisation light, and with 1.5 wt% CNTs, the radar absorption was 16 dB for the 9 mm composite thickness. However, at higher CNT loadings, the UV transmission depth in the photo resin was reduced due to poor dispersion and particle agglomeration phenomena. Another study that used CNTs was Cortés et al. [139], in which they explored the shape memory properties of PHEMA/PEGDA polymers, with a weight ratio of (3/1) using a DLP 3D printer (Table 1). They noticed that by including CNTs up to 0.5 wt% within methacrylate photo resin, the shape fixity and shape recovery reached ($R_f \approx 100\%$) and ($R_r > 95\%$) via Joule heating (Table 3), respectively, significantly improving electrically

triggered responses (Figure 22). The electrical conductivity and, thus, the possibility to remotely heat the nanocomposite was observed using the Joule effect.

Table 3. Shape memory properties of the DLP-printed nanocomposites (table reproduced from [139]).

Sample	CNT (wt%)	Direct Heating			Joule Heating		
		R_f (%)	R_r (%)	t_r (min)	R_f (%)	R_r (%)	t_r (min)
S0	-	≈100	99.1	7.7	-	-	-
S0.1	0.1	≈100	99.3	5.4	-	-	-
S0.3	0.3	≈100	98.3	5.5	≈100	98.7	3.4
S0.5	0.5	≈100	95.3	6.2	≈100	96.3	3.6

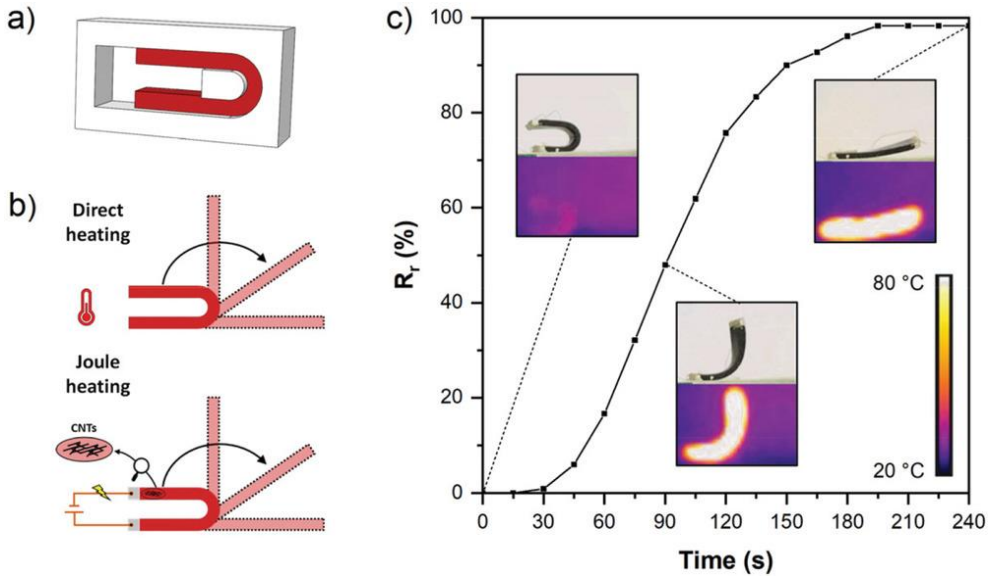

Figure 22. (**a**) DLP-printed mould to fix the U shape of CNT/methacrylate components; (**b**) direct heating and Joule heating to trigger the shape recovery; and (**c**) shape recovery under Joule heating using a thermal camera [139].

MWCNT nanocomposites can be incorporated as intelligent nanoparticles with stress sensitivity as well as a shape memory effect with improving electrical and thermal conductivity [245]. Mu et al. [64] employed MWCNT within a photocurable acrylic-based resin to produce conductive smart nanocomposite components using DLP 3DP (Figure 23). Electrical conductivity of 0.027 S/m was achieved with a 0.3 wt% loading of MWCNT. Shape memory properties were tested using ohmic heating (180 voltage) and 100% shape recovery was noticed in 20 s.

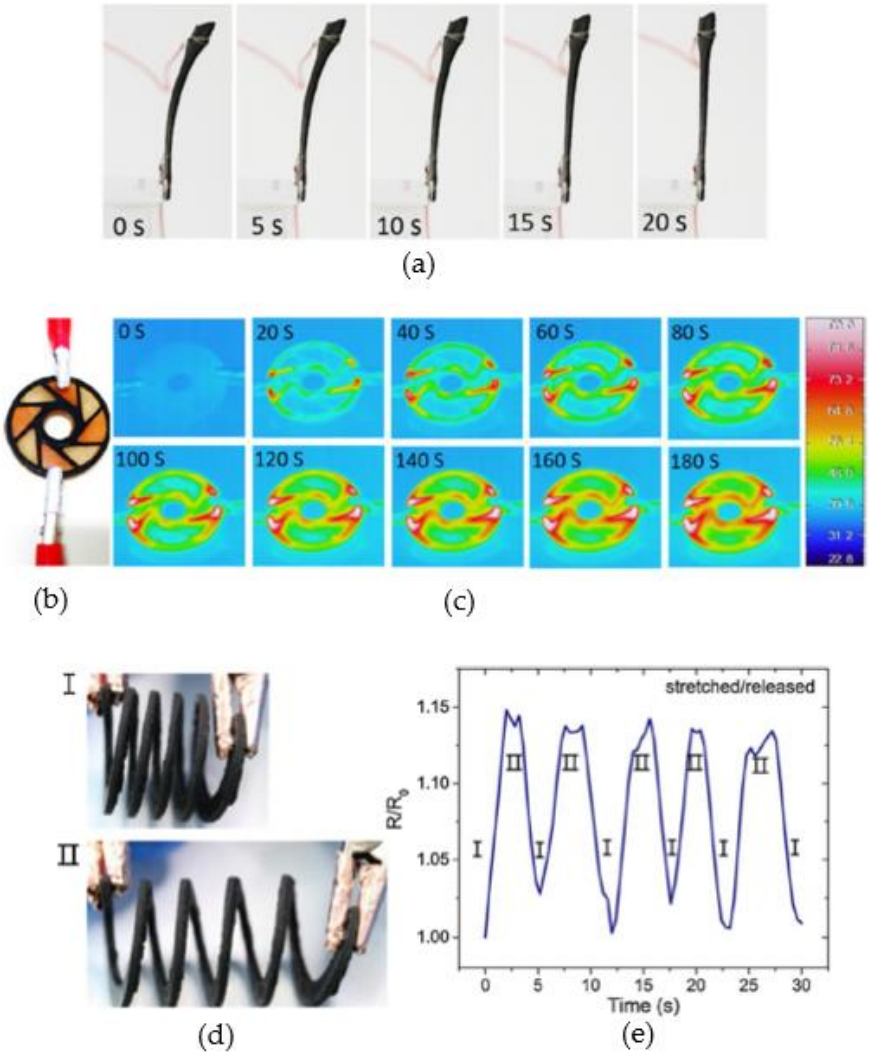

Figure 23. (**a**) Shape change of the sample during ohmic heating. (**b**) Optical image, (**c**) infrared images during heating. (**d**) Images of a stretchable spring structure in (I) released and (II) stretched. (**e**) Change in resistance of a representative gauge during five stretching/releasing cycles [64]. Copyright © 2022, Elsevier.

4.4.4. Graphene-Modified Polymeric Resin

Graphene is described as a multi-layer of a two-dimensional carbon nanofiller that appears as a honeycomb lattice, and the most known types are graphene nanoplatelets (GNPs) and graphene oxide (GO). Graphene can adsorb various atoms and molecules, which provide excellent toughness and modulus as well, as it has a potential aspect of research in the case of enhancing photopolymerisation and/or rheology of 3D-printed resins [246–248].

In their review, Guo et al. [237] clarified the outlines of using various AM technologies in the fabrication of graphene-based composites and presented the relationships among the fabrication process, required characterization methods, structural behaviour and applications of these composites. They also concluded that the 3DP of graphene-modified polymer composites attracted particular attention due to their high strength, excellent electrical and thermal conductivity and good shape-morphing behaviour. In addition, the authors presented that most 3D-printer techniques used to fabricate graphene-based composites are DIW, SLA and DLP. However, unlike SLA and DLP printers, DIW 3DP generally requires a complex post-treatment to evaporate the solvent. Hence, the SLA and DLP are more reliable methods due to their excellent resolution and unique interaction between

graphene and laser/UV light. Uysal [249] incorporated GO nanoparticles with contents of 0.05, 0.1, 0.15, 0.20 and 0.25 wt% to improve the tensile strength of epoxy/acrylate-based 3D-printed components via SLA, with a UV light source of 405 nm wavelength, and BAPO was used as a photoinitiator. It is noted that the morphological investigations indicated that the dispersion of GO was homogeneous without agglomeration after surface modifications by 3-(methacryloyloxy) propyl trimethoxysilane. Wang et al. [250] employed Formlabs Photopolymer standard resin (FLGPCL043D) via SLA, with a UV light source of 405 nm wavelength to enhance the 3DP of graphene-doped resin for laser desorption/ionization mass spectrometry analysis. They concluded that the 3DP process is rapid, simple and economical, resulting in excellent reusability and a long lifetime for the 3D-printed graphene nanocomposites. Chi et al. [191] explored DIW 3DP and recycling of graphene nanoplatelet (GNP)-filled commercial bisphenol epoxy components to develop a novel functional thixotropic agent that turns epoxy into shear-thinning printable ink. In addition, the inclusion of GNP up to 15 wt% exhibited increased thermal and electrical conductivity and improved thermo-induced shape memory performance (Figure 24). The recycled epoxy/GNP endowed the thixotropic agent to be prepared with new DIW resins. They also found that the 3D-printed components still have outstanding characteristics after multiple recycling cycles.

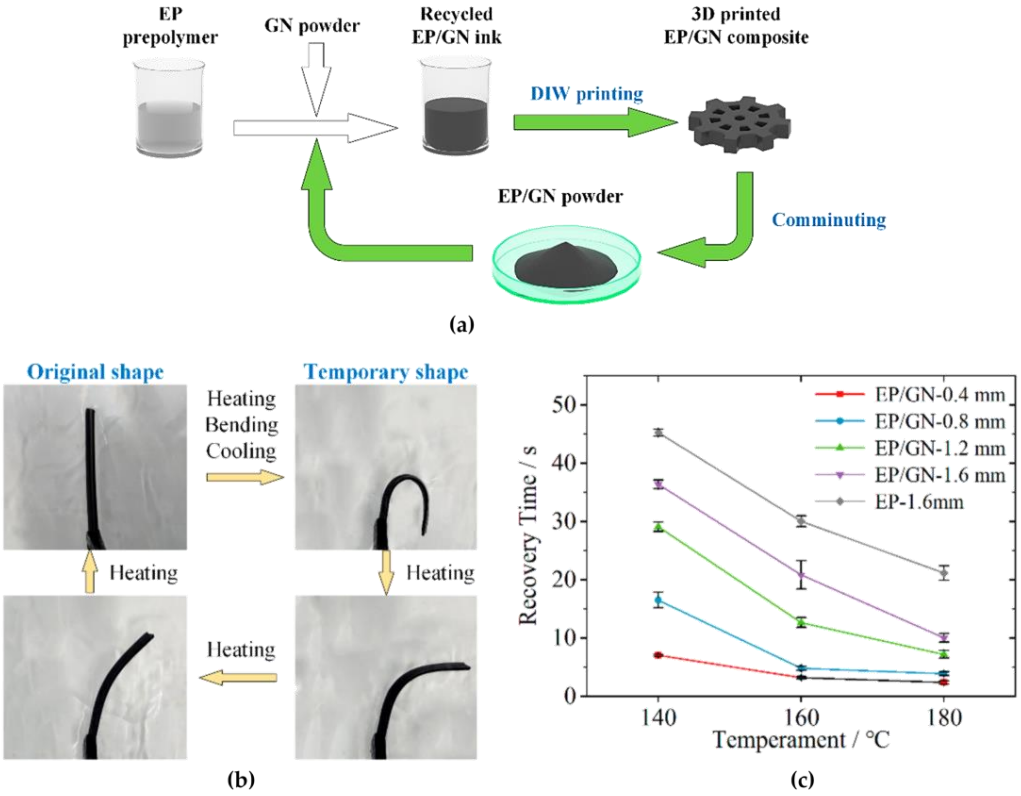

Figure 24. (**a**) Recycling of EP/GNP materials for DIW 3DP, (**b**) shape recovery process of a 3D-printed specimen, (**c**) shape recovery time of samples with different thicknesses at different temperatures [191]. Copyright © 2022, ACS.

Idowu et al. [192] manufactured GNP-reinforced shape memory polymer epoxy (SMPE) nanocomposites via a cryogenic sprayer system-assisted DIW. The authors concluded that the shape recovery, tensile strength and elastic modulus are increased by 15%, 17% and 30%, respectively, with an inclusion GNP of just 0.1 wt%. Further, the storage modulus and loss tangent are increased by 365% and 66%, respectively, with a GNP of 0.1 wt% compared to unfilled 3D-printed SMPE, indicating superior damping characteristics. Chowdhury [251] used a Micro-SLA 3D printer to fabricate graphene nanoparticles and modified the tBA resin with a crosslinker, diethylene glycol diacrylate (tBA-co-DEGDA).

It was reported that the inclusion of graphene nanoparticles of 0.1 and 0.3 wt% improved the shape fixity by 86.3%, with a recovery time of 6.95 s, with a printing speed of 90 mm/s. The author concluded that employing AM techniques for composite materials can create new prospects for designing novel materials.

4.5. Other Nanoparticle-Modified Polymeric Resin

Thus, 3D-printed nanocomposites are attracting more and more attention due to their advantages. So far, some other nanofillers are incorporated into 3D-printed polymeric resins, such as cellulose nanocrystals (CNCs), copper, zinc oxide nanoparticles (ZnONPs) and silver nanoparticles, which are crucial for realizing diverse 4DP applications. Below are some conclusions from these studies.

Kumar et al. [252] included CNC particles to reinforce stereolithographic resins (SLRs). The results showed that the storage modulus values are enhanced steadily with increasing CNC content for below and above T_g. A remarkable modulus improvement is noticed in the rubbery region by 166, 233 and 587% for CNC/SLR nanocomposites with CNC contents of 0.5, 1.0 and 5.0 wt%, respectively.

Bodkhe and Ermanni [193] employed piezoelectric barium titanate nanoparticles (BTNs) with contents of 0–30 wt% within a mixture ink of PLA, polyesteramide (PEA) and short carbon fibre, which were dissolved in dichloromethane (DCM) using DIW 3DP. The composite components exhibited good shape memory and sensing capabilities that resulted in a shape recovery of 95%, and the robust sensor could withstand temperatures ranging from 23 °C to 100 °C and to over 5000 operation cycles.

Lee et al. [253] prepared a methacrylate-based photoresin, including zinc oxide (ZnO) nanoparticles of 0, 3, 5, 7 and 9 wt% contents for DLP 3DP structures using 405 nm UV light, which enabled subsequent copper electroless plating (ELP). ZnO nanoparticles are added to the acrylate resin as catalytic seeds for ELP, and copper patterns are accurately added on 3DP ZnO. The strong adhesion between the copper layers and the surface of the 3D-printed structure was confirmed via an adhesion test. This technique can improve sensitivity to external stimuli such as an electromagnetic field for various applications, such as electronic devices and cardiovascular scaffolds. ZnO nanoparticles also attracted Siang et al. [122] to enhance the mechanical properties, printability and dimensional accuracy of acrylate-based photoresin. The authors indicated that ZnO could be considered as a photoinitiator in polymerization to facilitate layer curing in DLP 3DP with a 405 nm UV-light wavelength.

Wang et al. [169] prepared a novel resin via a DLP Pico2 printer containing gold nanoparticles (AuNPs) as a photothermal initiator with acrylate to form programmable light-activated 4DP SMPCs with tuneable transition temperatures that can be activated by light. The results show that the low-cost LED light is transformed into heat, which enables the shape transition at T_g of the polymer. The shape fixity and recovery ratios are improved to exceed 95%. In addition, the shape memory recovery results are predicted using numerical simulations. They also concluded that the presented approach can be useful for remotely controlling morphing, especially for the actuator and soft robotic applications.

Krivec et al. [254] reported a strategy to manufacture the construction of a simple radio frequency identification (RFID) package with an integrated surface acoustic wave transponder (SAW) via a multijet 3D printer. The resin consists of acrylate and 50 wt% of silver nanoparticles, in which the silver nanoparticle ink is used to fabricate the antenna for the wireless read-out. The SAW package prototype in a flip-chip configuration showed a significant signal-to-noise ratio (SNR) of about 30 dB via an antenna-bridged radio frequency link at a moderate distance of 3 cm. Ikram et al. [255] also reported the effects of silver nanoparticles on the physical and thermal behaviour of polymethylmethacrylate (PMMA) photopolymer resin using SLA 3DP. The study showed that the incorporation of silver 2 wt% improved the thermal stability by 6.6% and decreased weight loss by about 8%, compared to the unmodified resin.

4.6. Micro/Nanofibre-Modified Polymeric Resin

The 3DP of micro/nanofibre-reinforced polymeric composites promotes the development of SMPCs and broadens their applications, gaining more attention due to their versatile nature and variety of micro and complex structures. Hence, including micro/nanofibres within liquid-based resins can significantly improve the homogeneity, morphology, printability, thermal and mechanical properties, especially for material jetting and material extrusion techniques, thus, obtaining 3D-printed components with exceptional characteristics [2]. However, light-penetration depth in the photopolymerisation technique can be limited in 3DP to thin layers. This limitation, for instance, hinders the processing of fibre- and/or particle-reinforced polymeric composites due to scattering or blocking the UV or laser light and, consequently, impeding polymerization. Furthermore, the viscosity of the photopolymerisation resins should be within a range of 0.1 Pa·s to 10 Pa·s with low surface tension to lower the time of a new layer [39,111]. Thus, the compound resins' optical, rheological and chemical characteristics should be considered when selecting materials for liquid-based 3D printers. Below are some conclusions from these studies.

Hassan et al. [132] explored mechanical, thermal, electrical and shape memory properties of a methacrylate-based photoresin with the effect of including micro-carbonyl iron particles (CIPs) of 0.5 and 1 wt% via SLA 4DP. The photoresin consists of Butyl methacrylate monomer, crosslinker poly (ethylene glycol) dimethacrylate (PEGDMA), photoinitiator BAPO and CIP as a nano-modifier. The author concluded that the shape memory effect exhibited ratios of 99.95% and 99.89% for shape fixity and shape recovery, respectively. The thermal stability and mechanical characteristics are enhanced with the addition of CIPs.

Zhao et al. [256] explored the impact of including micro-aramid fibre (poly(p-benzoyl-p-phenylenediamine)) on plastic strengthening via 405 nm wavelength of DLP 3DP. The authors explain that viscosity and printability are perfect up to an aramid content of 7 wt%, and the photoresin is strengthened in the z-axis direction layer by layer. Further, they concluded that after dual curing of UV light and thermal curing, the tensile strength and modulus of the composite are 1.79- and 11.2-times, respectively, higher than those of the unreinforced resin.

Invernizzi et al. [257] presented carbon- and glass-fibre-reinforced multi-cure acrylate-based photoresin composites manufactured via UV-assisted 3DP. The results showed good 3D-printability macrostructures, thermal stability and mechanical properties that exhibited potential use in real-life structural applications. In another study, Guo et al. [189] investigated using short carbon fibres (SCFs) made from continuous carbon fibre (T300) as reinforcement for nanosilica/epoxy shape memory resin via DIW 3DP. The authors noted that including micro SCF of 25 wt% led to modifying rheological properties and improving the tensile strength and modulus to reach 100 MPa and 9 GPa, respectively, in addition to enhancing the printability by using three-roll milling in preparing the mixture ink.

Rodriguez et al. [197] developed a thermoset SMP mixture ink for DIW 3DP containing epoxidised soybean oil (EBSO) with bisphenol F diglycidyl ether (BFDGE) and carbon nanofibres (CNFs) as a filler material formed from graphitised cylindrical-shaped platelets with lengths of 20–200 μm and a diameter of 100 nm. EBSO is considered to be a renewable resource that can be 3D-printed with multi-material to fabricate lightweight complex structures, such as origami shape, and display programmable shape changes with time and temperature (Figure 25) that are triggered by thermal heating or electric (Joule) heating. They concluded that the 3DP of electrically conductive SMPs with fibre-based fillers could exhibit multiple shape changes actuated by heating of printed nanocomposites that can be considered for potential application for robotic medical and aerospace application devices.

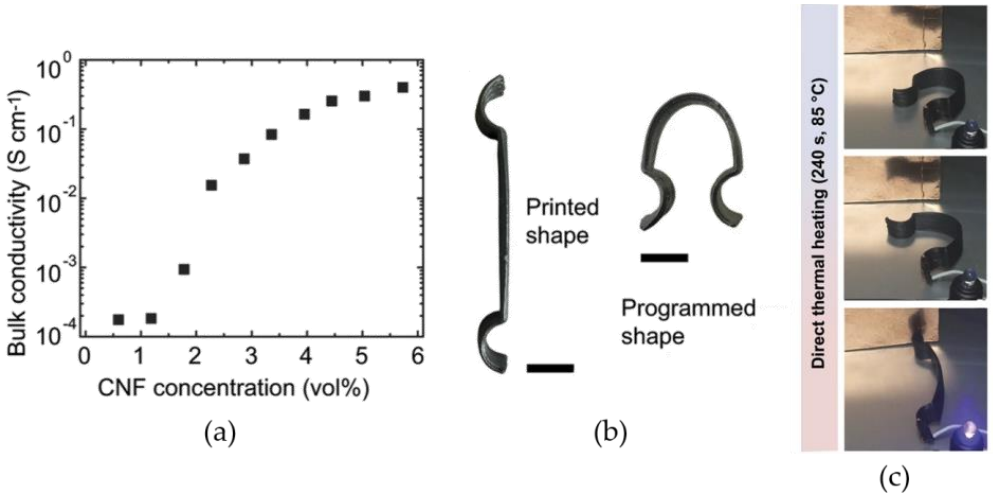

Figure 25. Electrical conductivity and multi-functionality of composite SMPs. (**a**) The plot of electrical conductivity dependence on CNF concentration where conductivity increases with increasing CNF concentration. (**b**) An electrically conductive (5.6 vol% CNF) part is shown in its printed or primary shape and its programmed shape. The component in (**b**) is connected to a power source and thermally actuated to change its form. A complete circuit in (**c**) where an LED become powered and lights up after 240 s at 80 °C [197].

Zhou et al. [258] incorporated nanocellulose in shape memory polyurethane (SMPU) to improve the thermomechanical characteristics of the porous SMPU via an innovative 3DP technique (Figure 26). This technique has sprayer and syringe pump parameters set at 120 mm/min and 30 µL/min, respectively. The cured printed components are subjected to solvent exchange by immersing in absolute alcohol, and then freeze-dried to obtain the SMPU composite components. The authors clarified that the shape fixity and shape recovery ratios are enhanced to above 99% by including cellulose nanocrystals (CNCs) and using ball-milled nanocellulose (BMC) (Table 4). In addition, the tensile strength of the 3D-printed SMPU composite is improved by 71% higher than unmodified PU. Further, they found that the composite T_g is close to human-body temperature, which enables potential applications in smart biomaterials.

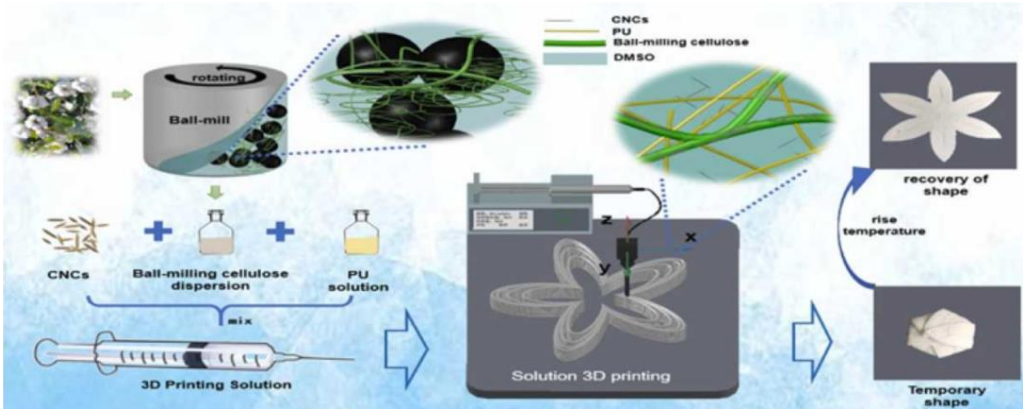

Figure 26. Diagram illustrates the 3DP of the shape memory nanocellulose/polyurethane composites [258].

Table 4. The shape fixation rate and shape recovery rate of the 3D-printed PU/nanocellulose shape memory composites compared with the pure PU (table reproduced from [258]).

Experiment No.	Sample	CNCs: BMC (in Weight)	R_f (%)	R_r (%)
1	PU	-	97.7 ± 0.8	96.9 ± 3.0
2	PU-1B	0.0: 1.0	98.1 ± 0.6	97.8 ± 2.0
3	PU-0.1C1B	0.1: 1.0	97.7 ± 0.1	99.7 ± 0.1
4	PU-0.3C1B	0.3: 1.0	98.1 ± 0.4	97.2 ± 0.2
5	PU-0.5C1B	0.5: 1.0	99.2 ± 0.6	98.9 ± 0.3
6	PU-1C1B	1.0: 1.0	99.4 ± 0.5	98.8 ± 0.4
7	PU-3C1B	3.0: 1.0	99.3 ± 0.8	99.4 ± 0.3
8	PU-5C1B	5.0: 1.0	99.7 ± 0.1	99.7 ± 1.6

5. Conclusions and Future Scope

In general, the progress in liquid-based 4D printing has developed significantly in the field of 3DP technology due to the variety and flexibility of selecting materials to produce high-accuracy and multifunctional shape memory components that can be used for different applications. Hence, with 3DP assistance, structure design would play a much more essential role in SMP/SMPC multifunctional applications to serve as shape-morphing, self-heal and self-assemble. Therefore, liquid-based additive manufacturing methods, such as vat photopolymerization, material jetting and DIW material extrusion, have become more popular 4DP techniques due to fine-tuning thermomechanical characteristics of SMPs/SMPCs to meet application demands. Thus, the overall terms (general, data, material) processing, features and applications for additive manufacturing were defined and described in accordance with ISO/ASTM 52900.

Prior to the new literature in this field, most of the smart resins used in the fabrication of 4D-printed components were acrylate-based and epoxy/acrylate-based resins. These resins can be combined to optimize several properties of their 4D-printed components, whereas some resins (photoresin) used commonly in 4DP, such as acrylic-based resin, offer high strain and quick cure. However, their samples display high shrinkage and a drop in mechanical properties. On the other hand, some resins (thermal cure) are brittle and slow cure and often require multi-cure, such as epoxy-based resin, despite their low shrinkage and high mechanical properties. Therefore, epoxy–acrylate resins can be optimised to produce SMPs/SMPCs appropriate for mechanically demanding applications.

There are several external stimuli for triggering the shape of smart dynamic structures, such as physical stimuli (light, electrical, magnetic), chemical stimuli (moisture/pH) and biological stimuli (biomolecule), that would greatly expand the applications of SMPs/SMPCs. However, the above review focused on temperature stimuli for shape memory polymers and their composites as thermal phase transitions that can be efficiently and effectively controlled.

Lastly, 3DP of polymer composites faces a challenge in liquid-based technologies as reinforcement micro/nanofibres or nanoparticles perhaps scatter or block light irradiation and restrict curing, especially for high content. Further, adding these fillers can increase the resin viscosity. Nevertheless, heating can decrease the viscosity to enhance the rheology and, thus, printability. Therefore, the 3D-printed nanocomposites can reimburse for the lack of mechanical characteristics from unmodified resins by including fillers.

Author Contributions: Conceptualization, M.A.; methodology, M.A.; resources, MA, D.M.D., C.T.M. and E.P.H.; writing—original draft preparation, M.A., V.F.M. and S.Z.; writing—review and editing, M.A., E.F., V.F.M., S.Z. and D.M.D.; visualization, M.A.; supervision, C.T.M., E.P.H. and D.M.D.; project administration, D.M.D.; funding acquisition, M.A., C.T.M. and D.M.D. All authors have read and agreed to the published version of the manuscript.

Funding: This research project is funded by Marie Skłodowska-Curie grant agreement No. 847577 cofounded by the European Regional Development Fund and Science Foundation Ireland (SFI) under Grant Number SFI/16/RC/3918 (Smart Manufacturing, Confirm Centre, UL).

Institutional Review Board Statement: Not applicable.

Informed Consent Statement: Not applicable.

Data Availability Statement: This review paper has used data previously published. The raw data required to reproduce those findings is available to download from the original publisher or authors of each reference. Further information can be provided on request.

Conflicts of Interest: The authors declare no conflict of interest.

Nomenclature

Nomenclature	
2PA	2-Phenoxyethyl Acrylate
4-MHHPA	Hexahydro-4-methylphthalic anhydride
BA	n-butyl acrylate
BF3	Boron trifluoride etherate
BGDGE	1,4-butanediol diglycidyl ether
Cyracure (UVI-6976)	Triarylsulfonium hexafluoroantimonate mixture salts
DGEDA	Bisphenol A diglycidyl ether diacrylate
DGEHBA	Diglycidyl ether of hydrogenated bisphenol A
DICY	Dicyandiamide
Diuron™	Dichlorophenyl urea
DPIHFP	Diphenyliodonium hexafluorophosphate
Ebecryl 8402	Aliphatic urethane diacrylate
ECC	3,4-Epoxy-cyclo hexylmethyl-3,4-epoxy-cyclohexane carboxylate
EGDGE	Ethylene glycol diglycidyl ether
EPOX	Methyl & 3,4-epoxycyclohexylcarboxylate
Esacure 1187	9-(4-Hydroxyethoxyphenyl) thiantrenium hexafluorophosphate
ETPTA	Ethoxylated trimethylolpropane triacrylate
GLYMO	3-glycidoxypropyltrimethoxysilane
IBOA	Isobornyl Acrylate
IPF	Bis(4-methylphenyl) iodonium hexafluorophosphate
Irgacure 184	1-hydroxycyclohexyl phenyl ketone
Irgacure 651	2,2-dimethoxy-2-methylpropiophenone
Irgacure 784	Bis(2,6-difluoro-3-(1-hydropyrrol-1-yl)phenyl) titanocene
Irgacure 1173	2-hydroxy-2-methylpropiophenone
MHHPA	Methylhexahydrophthalic anhydride
MJ	Material jetting
NGDGE	Neopentyl glycol diglycidyl ether
NMP	*N*-methyl-2-pyrrolidone
NVK	9-Vinylcarbazole
Omnirad 184	1-hydroxycyclohexyl phenyl ketone
OXT	3-ethyl-3-hydroxymethyl oxetane
PBN	Phenyl-N-tert-butylnitrone
PEG	Diglycidyl ether
PEGDA	Poly(ethylene glycol)diacrylate
PEO	Polyethylene oxide
PHEMA	Poly hydroxyethyl methacrylate
PLMC	Poly(D,I-lactide-co-trimethylene carbonate)
PUA	Aliphatic polyurethane acrylate
PVDF	Polyvinylidene fluoride
SMPCs	Shape memory polymer composites
SR349	Bisphenol A ethoxylate diacrylate
tBA	Tert-Butyl acrylate
TEGDMA	Triethylene glycol dimethacrylate
TMPTA	Trimethylolpropane triacrylate
TMPTA-EO3	Trimethylolpropane triacrylate
TMPEOTA	Trimethylolpropane ethoxylate triacrylate
TPGDA	Tripropylene glycol diacrylate
TPO-L	Ethyl(2,4,6-trimethylbenzoyl) phenyl phosphinate
TPO	Diphenyl(2,4,6-trimethylbenzoyl) phosphine oxide
Tris	Tris(hydroxymethyl) aminomethane
ZnTPP	Zinc Tetraphenylporphyrin
NMP	*N*-methyl-2-pyrrolidone
NMP	*N*-methyl-2-pyrrolidone

References

1. American Society for Testing and Materials American Society for Testing and Materials. ISO/ASTM52900:21 Additive Manufacturing—General Principles—Fundamentals and Vocabulary. *Addit. Manuf. Gen. Princ.* **2021**, *i*, 1–9.
2. Subash, A.; Kandasubramanian, B. 4D Printing of Shape Memory Polymers. *Eur. Polym. J.* **2020**, *134*, 109771. [CrossRef]
3. Yuan, C.; Lu, T.; Wang, T.J. Mechanics-Based Design Strategies for 4D Printing: A Review. *Forces Mech.* **2022**, *7*, 100081. [CrossRef]
4. Dimassi, S.; Demoly, F.; Cruz, C.; Qi, H.J.; Kim, K.-Y.; André, J.-C.; Gomes, S. An Ontology-Based Framework to Formalize and Represent 4D Printing Knowledge in Design. *Comput. Ind.* **2021**, *126*, 103374. [CrossRef]
5. Li, H.; Gao, X.; Luo, Y. Multi-Shape Memory Polymers Achieved by the Spatio-Assembly of 3D Printable Thermoplastic Building Blocks. *Soft Matter* **2016**, *12*, 3226–3233. [CrossRef] [PubMed]

6. Roppolo, I.; Chiappone, A.; Angelini, A.; Stassi, S.; Frascella, F.; Pirri, C.F.; Ricciardi, C.; Descrovi, E. 3D Printable Light-Responsive Polymers. *Mater. Horiz.* **2017**, *4*, 396–401. [CrossRef]
7. Simińska-Stanny, J.; Nizioł, M.; Szymczyk-Ziółkowska, P.; Brożyna, M.; Junka, A.; Shavandi, A.; Podstawczyk, D. 4D Printing of Patterned Multimaterial Magnetic Hydrogel Actuators. *Addit. Manuf.* **2022**, *49*, 102506. [CrossRef]
8. Khalid, M.Y.; Arif, Z.U.; Noroozi, R.; Zolfagharian, A.; Bodaghi, M. 4D Printing of Shape Memory Polymer Composites: A Review on Fabrication Techniques, Applications, and Future Perspectives. *J. Manuf. Process.* **2022**, *81*, 759–797. [CrossRef]
9. Sheikh, A.; Abourehab, M.A.S.; Kesharwani, P. The Clinical Significance of 4D Printing. *Drug Discov. Today* **2023**, *28*, 103391. [CrossRef]
10. Wan, X.; He, Y.; Liu, Y.; Leng, J. 4D Printing of Multiple Shape Memory Polymer and Nanocomposites with Biocompatible, Programmable and Selectively Actuated Properties. *Addit. Manuf.* **2022**, *53*, 102689. [CrossRef]
11. Chen, Q.; Sukmanee, T.; Rong, L.; Yang, M.; Ren, J.; Ekgasit, S.; Advincula, R. A Dual Approach in Direct Ink Writing of Thermally Cured Shape Memory Rubber Toughened Epoxy. *ACS Appl. Polym. Mater.* **2020**, *2*, 5492–5500. [CrossRef]
12. Wei, P.; Leng, H.; Chen, Q.; Advincula, R.C.; Pentzer, E.B. Reprocessable 3D-Printed Conductive Elastomeric Composite Foams for Strain and Gas Sensing. *ACS Appl. Polym. Mater.* **2019**, *1*, 885–892. [CrossRef]
13. Alo, O.A.; Mauchline, D.; Otunniyi, I.O. 3D-Printed Functional Polymers and Nanocomposites: Defects Characterization and Product Quality Improvement. *Adv. Eng. Mater.* **2022**, *24*, 2101219. [CrossRef]
14. Rodríguez-Pombo, L.; Xu, X.; Seijo-Rabina, A.; Ong, J.J.; Alvarez-Lorenzo, C.; Rial, C.; Nieto, D.; Gaisford, S.; Basit, A.W.; Goyanes, A. Volumetric 3D Printing for Rapid Production of Medicines. *Addit. Manuf.* **2022**, *52*, 102673. [CrossRef]
15. Bao, Y. Recent Trends in Advanced Photoinitiators for Vat Photopolymerization 3D Printing. *Macromol. Rapid Commun.* **2022**, *43*, 2200202. [CrossRef]
16. Nechausov, S.; Ivanchenko, A.; Morozov, O.; Miriyev, A.; Must, I.; Platnieks, O.; Jurinovs, M.; Gaidukovs, S.; Aabloo, A.; Kovač, M.; et al. Effects of Ionic Liquids and Dual Curing on Vat Photopolymerization Process and Properties of 3d-Printed Ionogels. *Addit. Manuf.* **2022**, *56*, 102895. [CrossRef]
17. O'Connor, H.J.; Dickson, A.N.; Dowling, D.P. Evaluation of the Mechanical Performance of Polymer Parts Fabricated Using a Production Scale Multi Jet Fusion Printing Process. *Addit. Manuf.* **2018**, *22*, 381–387. [CrossRef]
18. Yu, K.; Dunn, M.L.; Qi, H.J. Digital Manufacture of Shape Changing Components. *Extrem. Mech. Lett.* **2015**, *4*, 9–17. [CrossRef]
19. Tyagi, S.; Yadav, A.; Deshmukh, S. Review on Mechanical Characterization of 3D Printed Parts Created Using Material Jetting Process. *Mater. Today Proc.* **2021**, *51*, 1012–1016. [CrossRef]
20. Gülcan, O.; Günaydın, K.; Tamer, A. The State of the Art of Material Jetting—A Critical Review. *Polymers* **2021**, *13*, 2829. [CrossRef]
21. Saadi, M.A.S.R.; Maguire, A.; Pottackal, N.T.; Thakur, M.S.H.; Ikram, M.M.; Hart, A.J.; Ajayan, P.M.; Rahman, M.M. Direct Ink Writing: A 3D Printing Technology for Diverse Materials. *Adv. Mater.* **2022**, *34*, 2108855. [CrossRef] [PubMed]
22. Lim, G.J.H.; Yang, Z.; Hou, Y.; Sugumaran, P.J.; Qiao, Z.; Ding, J.; Yan, W.; Yang, Y. Direct Ink Writing for High-Efficiency Microwave Attenuation with Nanofibers Alignment. *ACS Appl. Mater. Interfaces* **2022**, *14*, 31267–31276. [CrossRef] [PubMed]
23. Huang, T.; Liu, W.; Su, C.; Li, Y.; Sun, J. Direct Ink Writing of Conductive Materials for Emerging Energy Storage Systems. *Nano Res.* **2022**, *15*, 6091–6111. [CrossRef]
24. Del Barrio, J.; Sánchez-Somolinos, C. Light to Shape the Future: From Photolithography to 4D Printing. *Adv. Opt. Mater.* **2019**, *7*. [CrossRef]
25. Pierau, L.; Elian, C.; Akimoto, J.; Ito, Y.; Caillol, S.; Versace, D.L. Bio-Sourced Monomers and Cationic Photopolymerization–The Green Combination towards Eco-Friendly and Non-Toxic Materials. *Prog. Polym. Sci.* **2022**, *127*, 101517. [CrossRef]
26. Chaudhary, R.; Fabbri, P.; Leoni, E.; Mazzanti, F.; Akbari, R.; Antonini, C. Additive Manufacturing by Digital Light Processing: A Review. *Prog. Addit. Manuf.* **2022**, *2022*, 1–21. [CrossRef]
27. Bongiovanni, R.; Vitale, A. Vat Photopolymerization. In *High Resolution Manufacturing from 2D to 3D/4D Printing*; Springer: Berlin/Heidelberg, Germany, 2022; pp. 17–46. [CrossRef]
28. Müller, S.M.; Schlögl, S.; Wiesner, T.; Haas, M.; Griesser, T. Recent Advances in Type I Photoinitiators for Visible Light Induced Photopolymerization. *ChemPhotoChem* **2022**, *2022*, e202200091. [CrossRef]
29. Kauppila, I. What Is Material Jetting?—3D Printing Basics. Available online: https://all3dp.com/1/what-is-material-jetting-3d-printing-basics/ (accessed on 27 December 2022).
30. O'Neill, P.; Jolivet, L.; Kent, N.J.; Brabazon, D. Physical Integrity of 3D Printed Parts for Use as Embossing Tools. *Adv. Mater. Process. Technol.* **2017**, *3*, 308–317. [CrossRef]
31. Rayate, A.; Jain, P.K. A Review on 4D Printing Material Composites and Their Applications. *Mater. Today Proc.* **2018**, *5*, 20474–20484. [CrossRef]
32. Xu, W.; Jambhulkar, S.; Zhu, Y.; Ravichandran, D.; Kakarla, M.; Vernon, B.; Lott, D.G.; Cornella, J.L.; Shefi, O.; Miquelard-Garnier, G.; et al. 3D Printing for Polymer/Particle-Based Processing: A Review. *Compos. Part B Eng.* **2021**, *223*, 109102. [CrossRef]
33. Abdulhameed, O.; Al-Ahmari, A.; Ameen, W.; Mian, S.H. Additive Manufacturing: Challenges, Trends, and Applications. *Adv. Mech. Eng.* **2019**, *11*, 168781401882288. [CrossRef]
34. Kafle, A.; Luis, E.; Silwal, R.; Pan, H.M.; Shrestha, P.L.; Bastola, A.K. 3D/4D Printing of Polymers: Fused Deposition Modelling (FDM), Selective Laser Sintering (SLS), and Stereolithography (SLA). *Polymers* **2021**, *13*, 3101. [CrossRef] [PubMed]
35. Dilberoglu, U.M.; Gharehpapagh, B.; Yaman, U.; Dolen, M. The Role of Additive Manufacturing in the Era of Industry 4.0. *Procedia Manuf.* **2017**, *11*, 545–554. [CrossRef]

36. Rastogi, P.; Kandasubramanian, B. Breakthrough in the Printing Tactics for Stimuli-Responsive Materials: 4D Printing. *Chem. Eng. J.* **2019**, *366*, 264–304. [CrossRef]
37. Löwa, N.; Fabert, J.-M.; Gutkelch, D.; Paysen, H.; Kosch, O.; Wiekhorst, F. 3D-Printing of Novel Magnetic Composites Based on Magnetic Nanoparticles and Photopolymers. *J. Magn. Magn. Mater.* **2019**, *469*, 456–460. [CrossRef]
38. Joshi, S.; Rawat, K.; Karunakaran, C.; Rajamohan, V.; Mathew, A.T.; Koziol, K.; Kumar Thakur, V.; Balan, A.S.S. 4D Printing of Materials for the Future: Opportunities and Challenges. *Appl. Mater. Today* **2020**, *18*, 100490. [CrossRef]
39. Andreu, A.; Su, P.-C.; Kim, J.-H.; Ng, C.S.; Kim, S.; Kim, I.; Lee, J.; Noh, J.; Subramanian, A.S.; Yoon, Y.-J. 4D Printing Materials for Vat Photopolymerization. *Addit. Manuf.* **2021**, *44*, 102024. [CrossRef]
40. Hu, G.; Cao, Z.; Hopkins, M.; Hayes, C.; Daly, M.; Zhou, H.; Devine, D.M. Optimizing the Hardness of SLA Printed Objects by Using the Neural Network and Genetic Algorithm. *Procedia Manuf.* **2019**, *38*, 117–124. [CrossRef]
41. Robles Martinez, P.; Basit, A.W.; Gaisford, S. *The History, Developments and Opportunities of Stereolithography*; Springer: Berlin/Heidelberg, Germany, 2018; pp. 55–79.
42. Singh, S.; Ramakrishna, S.; Singh, R. Material Issues in Additive Manufacturing: A Review. *J. Manuf. Process.* **2017**, *25*, 185–200. [CrossRef]
43. Bagheri, A.; Jin, J. Photopolymerization in 3D Printing. *ACS Appl. Polym. Mater.* **2019**, *1*, 593–611. [CrossRef]
44. Ding, N.; Wu, Y.; Xu, W.; Lyu, J.; Wang, Y.; Zi, L.; Shao, L.; Sun, R.; Wang, N.; Liu, S.; et al. A Novel Approach for Designing Efficient Broadband Photodetectors Expanding from Deep Ultraviolet to near Infrared. *Light Sci. Appl.* **2022**, *11*, 91. [CrossRef] [PubMed]
45. Melchels, F.P.W.; Feijen, J.; Grijpma, D.W. A Review on Stereolithography and Its Applications in Biomedical Engineering. *Biomaterials* **2010**, *31*, 6121–6130. [CrossRef] [PubMed]
46. Ligon, S.C.; Liska, R.; Stampfl, J.; Gurr, M.; Mülhaupt, R. Polymers for 3D Printing and Customized Additive Manufacturing. *Chem. Rev.* **2017**, *117*, 10212–10290. [CrossRef] [PubMed]
47. Hu, G.; Cao, Z.; Hopkins, M.; Lyons, J.G.; Brennan-Fournet, M.; Devine, D.M. Nanofillers Can Be Used to Enhance the Thermal Conductivity of Commercially Available SLA Resins. *Procedia Manuf.* **2019**, *38*, 1236–1243. [CrossRef]
48. Moritz, V.F.; Bezerra, G.S.N.; Hopkins, M., Jr.; Fuenmayor, E.; Günbay, S.; Hayes, C.; Lyons, J.G.; Devine, D.M. Heat Dissipation Plays Critical Role for Longevity of Polymer-Based 3D-Printed Inserts for Plastics Injection Moulding. *J. Manuf. Mater. Process.* **2022**, *6*, 117. [CrossRef]
49. Choong, Y.Y.C.; Maleksaeedi, S.; Eng, H.; Wei, J.; Su, P.C. 4D Printing of High Performance Shape Memory Polymer Using Stereolithography. *Mater. Des.* **2017**, *126*, 219–225. [CrossRef]
50. Yu, R.; Yang, X.; Zhang, Y.; Zhao, X.; Wu, X.; Zhao, T.; Zhao, Y.; Huang, W. Three-Dimensional Printing of Shape Memory Composites with Epoxy-Acrylate Hybrid Photopolymer. *ACS Appl. Mater. Interfaces* **2017**, *9*, 1820–1829. [CrossRef]
51. Zhao, T.; Yu, R.; Li, X.; Cheng, B.; Zhang, Y.; Yang, X.; Zhao, X.; Zhao, Y.; Huang, W. 4D Printing of Shape Memory Polyurethane via Stereolithography. *Eur. Polym. J.* **2018**, *101*, 120–126. [CrossRef]
52. Inverardi, N.; Pandini, S.; Bignotti, F.; Scalet, G.; Marconi, S.; Auricchio, F. Sequential Motion of 4D Printed Photopolymers with Broad Glass Transition. *Macromol. Mater. Eng.* **2020**, *305*, 1900370. [CrossRef]
53. Credi, C.; Fiorese, A.; Tironi, M.; Bernasconi, R.; Magagnin, L.; Levi, M.; Turri, S. 3D Printing of Cantilever-Type Microstructures by Stereolithography of Ferromagnetic Photopolymers. *ACS Appl. Mater. Interfaces* **2016**, *8*, 26332–26342. [CrossRef]
54. Deng, D.; Jain, A.; Yodvanich, N.; Araujo, A.; Chen, Y. Three-Dimensional Circuit Fabrication Using Four-Dimensional Printing and Direct Ink Writing. In Proceedings of the 2016 International Symposium on Flexible Automation (ISFA), Cleveland, OH, USA, 1–3 August 2016; pp. 286–291.
55. Ge, Q.; Sakhaei, A.H.; Lee, H.; Dunn, C.K.; Fang, N.X.; Dunn, M.L. Multimaterial 4D Printing with Tailorable Shape Memory Polymers. *Sci. Rep.* **2016**, *6*, 31110. [CrossRef]
56. Del Pozo, M.; Delaney, C.; Pilz da Cunha, M.; Debije, M.G.; Florea, L.; Schenning, A.P.H.J. Temperature-Responsive 4D Liquid Crystal Microactuators Fabricated by Direct Laser Writing by Two-Photon Polymerization. *Small Struct.* **2022**, *3*, 2100158. [CrossRef]
57. Zhao, Z.; Tian, X.; Song, X. Engineering Materials with Light: Recent Progress in Digital Light Processing Based 3D Printing. *J. Mater. Chem. C* **2020**, *8*, 13896–13917. [CrossRef]
58. Lantean, S.; Barrera, G.; Pirri, C.F.; Tiberto, P.; Sangermano, M.; Roppolo, I.; Rizza, G. 3D Printing of Magnetoresponsive Polymeric Materials with Tunable Mechanical and Magnetic Properties by Digital Light Processing. *Adv. Mater. Technol.* **2019**, *4*, 1900505. [CrossRef]
59. Nagarajan, B.; Mertiny, P.; Qureshi, A.J. Magnetically Loaded Polymer Composites Using Stereolithography—Material Processing and Characterization. *Mater. Today Commun.* **2020**, *25*, 101520. [CrossRef]
60. Stassi, S.; Fantino, E.; Calmo, R.; Chiappone, A.; Gillono, M.; Scaiola, D.; Pirri, C.F.; Ricciardi, C.; Chiadò, A.; Roppolo, I. Polymeric 3D Printed Functional Microcantilevers for Biosensing Applications. *ACS Appl. Mater. Interfaces* **2017**, *9*, 19193–19201. [CrossRef]
61. Zarek, M.; Layani, M.; Cooperstein, I.; Sachyani, E.; Cohn, D.; Magdassi, S. 3D Printing of Shape Memory Polymers for Flexible Electronic Devices. *Adv. Mater.* **2016**, *28*, 4449–4454. [CrossRef] [PubMed]
62. Ge, L.; Dong, L.; Wang, D.; Ge, Q.; Gu, G. A Digital Light Processing 3D Printer for Fast and High-Precision Fabrication of Soft Pneumatic Actuators. *Sens. Actuators A Phys.* **2018**, *273*, 285–292. [CrossRef]

63. Choong, Y.Y.C.; Maleksaeedi, S.; Eng, H.; Yu, S.; Wei, J.; Su, P.C. High Speed 4D Printing of Shape Memory Polymers with Nanosilica. *Appl. Mater. Today* **2020**, *18*, 100515. [CrossRef]
64. Mu, Q.; Wang, L.; Dunn, C.K.; Kuang, X.; Duan, F.; Zhang, Z.; Qi, H.J.; Wang, T. Digital Light Processing 3D Printing of Conductive Complex Structures. *Addit. Manuf.* **2017**, *18*, 74–83. [CrossRef]
65. Devillard, C.D.; Mandon, C.A.; Lambert, S.A.; Blum, L.J.; Marquette, C.A. Bioinspired Multi-Activities 4D Printing Objects: A New Approach Toward Complex Tissue Engineering. *Biotechnol. J.* **2018**, *13*, 1800098. [CrossRef] [PubMed]
66. Spiegel, C.A.; Hackner, M.; Bothe, V.P.; Spatz, J.P.; Blasco, E. 4D Printing of Shape Memory Polymers: From Macro to Micro. *Adv. Funct. Mater.* **2022**, *32*, 2110580. [CrossRef]
67. Zhakeyev, A.; Zhang, L.; Xuan, J. Photoactive Resin Formulations and Composites for Optical 3D and 4D Printing of Functional Materials and Devices. In *3D and 4D Printing of Polymer Nanocomposite Materials: Processes, Applications, and Challenges*; Elsevier: Amsterdam, The Netherlands, 2019; pp. 387–425. ISBN 9780128168059.
68. Kuang, X.; Roach, D.J.; Wu, J.; Hamel, C.M.; Ding, Z.; Wang, T.; Dunn, M.L.; Qi, H.J. Advances in 4D Printing: Materials and Applications. *Adv. Funct. Mater.* **2019**, *29*, 1805290. [CrossRef]
69. Huang, J.; Qin, Q.; Wang, J. A Review of Stereolithography: Processes and Systems. *Processes* **2020**, *8*, 1138. [CrossRef]
70. Yeow, J.; Chapman, R.; Gormley, A.J.; Boyer, C. Up in the Air: Oxygen Tolerance in Controlled/Living Radical Polymerisation. *Chem. Soc. Rev.* **2018**, *47*, 4357–4387. [CrossRef]
71. Ligon, S.C.; Husár, B.; Wutzel, H.; Holman, R.; Liska, R. Strategies to Reduce Oxygen Inhibition in Photoinduced Polymerization. *Chem. Rev.* **2014**, *114*, 557–589. [CrossRef]
72. Janusziewicz, R.; Tumbleston, J.R.; Quintanilla, A.L.; Mecham, S.J.; DeSimone, J.M. Layerless Fabrication with Continuous Liquid Interface Production. *Proc. Natl. Acad. Sci. USA* **2016**, *113*, 11703–11708. [CrossRef]
73. Tumbleston, J.R.; Shirvanyants, D.; Ermoshkin, N.; Janusziewicz, R.; Johnson, A.R.; Kelly, D.; Chen, K.; Pinschmidt, R.; Rolland, J.P.; Ermoshkin, A.; et al. Continuous Liquid Interface Production of 3D Objects. *Science* **2015**, *347*, 1349–1352. [CrossRef]
74. Ware, H.O.T.; Sun, C. Method for Attaining Dimensionally Accurate Conditions for High-Resolution Three-Dimensional Printing Ceramic Composite Structures Using MicroCLIP Process. *J. Micro Nano-Manuf.* **2019**, *7*, 031001. [CrossRef]
75. Mohamed, M.; Kumar, H.; Wang, Z.; Martin, N.; Mills, B.; Kim, K. Rapid and Inexpensive Fabrication of Multi-Depth Microfluidic Device Using High-Resolution LCD Stereolithographic 3D Printing. *J. Manuf. Mater. Process.* **2019**, *3*, 26. [CrossRef]
76. Shan, W.; Chen, Y.; Hu, M.; Qin, S.; Liu, P. 4D Printing of Shape Memory Polymer via Liquid Crystal Display (LCD) Stereolithographic 3D Printing. *Mater. Res. Express* **2020**, *7*, 105305. [CrossRef]
77. Kholkhoev, B.C.; Bardakova, K.N.; Epifanov, E.O.; Matveev, Z.A.; Shalygina, T.A.; Atutov, E.B.; Voronina, S.Y.; Timashev, P.S.; Burdukovskii, V.F. A Photosensitive Composition Based on an Aromatic Polyamide for LCD 4D Printing of Shape Memory Mechanically Robust Materials. *Chem. Eng. J.* **2023**, *454*, 140423. [CrossRef]
78. Loh, G.H.; Pei, E.; Harrison, D.; Monzón, M.D. An Overview of Functionally Graded Additive Manufacturing. *Addit. Manuf.* **2018**, *23*, 34–44. [CrossRef]
79. Salcedo, E.; Baek, D.; Berndt, A.; Ryu, J.E. Simulation and Validation of Three Dimension Functionally Graded Materials by Material Jetting. *Addit. Manuf.* **2018**, *22*, 351–359. [CrossRef]
80. Yu, K.; Ritchie, A.; Mao, Y.; Dunn, M.L.; Qi, H.J. Controlled Sequential Shape Changing Components by 3D Printing of Shape Memory Polymer Multimaterials. *Procedia IUTAM* **2015**, *12*, 193–203. [CrossRef]
81. Tee, Y.L.; Tran, P.; Leary, M.; Pille, P.; Brandt, M. 3D Printing of Polymer Composites with Material Jetting: Mechanical and Fractographic Analysis. *Addit. Manuf.* **2020**, *36*, 101558. [CrossRef]
82. Yap, Y.L.; Wang, C.; Sing, S.L.; Dikshit, V.; Yeong, W.Y.; Wei, J. Material Jetting Additive Manufacturing: An Experimental Study Using Designed Metrological Benchmarks. *Precis. Eng.* **2017**, *50*, 275–285. [CrossRef]
83. Kim, S. Electronic Ink Formulation for Drop-on-Demand (DoD) Inkjet Printing Fabrication Process. In Proceedings of the 2019 34th International Technical Conference on Circuits/Systems, Computers and Communications (ITC-CSCC), Jeju, Republic of Korean, 23–26 June 2019; pp. 1–2.
84. Shah, M.A.; Lee, D.-G.; Lee, B.-Y.; Hur, S. Classifications and Applications of Inkjet Printing Technology: A Review. *IEEE Access* **2021**, *9*, 140079–140102. [CrossRef]
85. Mora, S.; Pugno, N.M.; Misseroni, D. 3D Printed Architected Lattice Structures by Material Jetting. *Mater. Today* **2022**, *59*, 107–132. [CrossRef]
86. Patpatiya, P.; Chaudhary, K.; Shastri, A.; Sharma, S. A Review on Polyjet 3D Printing of Polymers and Multi-Material Structures. *Proc. Inst. Mech. Eng. Part C J. Mech. Eng. Sci.* **2022**, *236*, 7899–7926. [CrossRef]
87. Chadha, C.; Olaivar, G.; Patterson, A.E.; Jasiuk, I.M. Design for Multi-Material Manufacturing Using Polyjet Printing Process: A Review. In Proceedings of the 27th Design for Manufacturing and the Life Cycle Conference (DFMLC), St. Louis, MO, USA, 14–17 August 2022; Volume 5.
88. Sireesha, M.; Lee, J.; Kranthi Kiran, A.S.; Babu, V.J.; Kee, B.B.T.; Ramakrishna, S. A Review on Additive Manufacturing and Its Way into the Oil and Gas Industry. *RSC Adv.* **2018**, *8*, 22460–22468. [CrossRef]
89. Phung, T.H.; Kwon, K.-S. Improved Continuous Inkjet for Selective Area Coating Using High-Viscosity Insulating Inks. *Adv. Eng. Mater.* **2022**, *24*, 2101527. [CrossRef]
90. Freire, E.M. Ink Jet Printing Technology (CIJ/DOD). In *Digital Printing of Textiles*; Elsevier: Amsterdam, The Netherlands, 2006; pp. 29–52.

91. Kholghi Eshkalak, S.; Chinnappan, A.; Jayathilaka, W.A.D.M.; Khatibzadeh, M.; Kowsari, E.; Ramakrishna, S. A Review on Inkjet Printing of CNT Composites for Smart Applications. *Appl. Mater. Today* **2017**, *9*, 372–386. [CrossRef]
92. Elkaseer, A.; Chen, K.J.; Janhsen, J.C.; Refle, O.; Hagenmeyer, V.; Scholz, S.G. Material Jetting for Advanced Applications: A State-of-the-Art Review, Gaps and Future Directions. *Addit. Manuf.* **2022**, *60*, 103270. [CrossRef]
93. Ameta, K.L.; Solanki, V.S.; Singh, V.; Devi, A.P.; Chundawat, R.S.; Haque, S. Critical Appraisal and Systematic Review of 3D & 4D Printing in Sustainable and Environment-Friendly Smart Manufacturing Technologies. *Sustain. Mater. Technol.* **2022**, *34*, e00481. [CrossRef]
94. Elkaseer, A.; Schneider, S.; Deng, Y.; Scholz, S.G. Effect of Process Parameters on the Performance of Drop-On-Demand 3D Inkjet Printing: Geometrical-Based Modeling and Experimental Validation. *Polymers* **2022**, *14*, 2557. [CrossRef] [PubMed]
95. Rafiee, M.; Farahani, R.D.; Therriault, D. Multi-Material 3D and 4D Printing: A Survey. *Adv. Sci.* **2020**, *7*, 1–26. [CrossRef]
96. Ching, T.; Li, Y.; Karyappa, R.; Ohno, A.; Toh, Y.-C.; Hashimoto, M. Fabrication of Integrated Microfluidic Devices by Direct Ink Writing (DIW) 3D Printing. *Sens. Actuators B Chem.* **2019**, *297*, 126609. [CrossRef]
97. Zhang, Y.; Zhang, F.; Yan, Z.; Ma, Q.; Li, X.; Huang, Y.; Rogers, J.A. Printing, Folding and Assembly Methods for Forming 3D Mesostructures in Advanced Materials. *Nat. Rev. Mater.* **2017**, *2*, 17019. [CrossRef]
98. Yang, G.; Sun, Y.; Limin, Q.; Li, M.; Ou, K.; Fang, J.; Fu, Q. Direct-Ink-Writing (DIW) 3D Printing Functional Composite Materials Based on Supra-Molecular Interaction. *Compos. Sci. Technol.* **2021**, *215*, 109013. [CrossRef]
99. Zhao, J.; Zhang, Y.; Zhao, X.; Wang, R.; Xie, J.; Yang, C.; Wang, J.; Zhang, Q.; Li, L.; Lu, C.; et al. Direct Ink Writing of Adjustable Electrochemical Energy Storage Device with High Gravimetric Energy Densities. *Adv. Funct. Mater.* **2019**, *29*, 1900809. [CrossRef]
100. Murphy, S.V.; Atala, A. 3D Bioprinting of Tissues and Organs. *Nat. Biotechnol.* **2014**, *32*, 773–785. [CrossRef]
101. Li, V.C.-F.; Dunn, C.K.; Zhang, Z.; Deng, Y.; Qi, H.J. Direct Ink Write (DIW) 3D Printed Cellulose Nanocrystal Aerogel Structures. *Sci. Rep.* **2017**, *7*, 8018. [CrossRef] [PubMed]
102. Seyedsalehi, A.; Daneshmandi, L.; Barajaa, M.; Riordan, J.; Laurencin, C.T. Fabrication and Characterization of Mechanically Competent 3D Printed Polycaprolactone-Reduced Graphene Oxide Scaffolds. *Sci. Rep.* **2020**, *10*, 22210. [CrossRef]
103. Daneshmandi, L.; Holt, B.D.; Arnold, A.M.; Laurencin, C.T.; Sydlik, S.A. Ultra-Low Binder Content 3D Printed Calcium Phosphate Graphene Scaffolds as Resorbable, Osteoinductive Matrices That Support Bone Formation in Vivo. *Sci. Rep.* **2022**, *12*, 6960. [CrossRef] [PubMed]
104. Cheng, Y.; Chan, K.H.; Wang, X.-Q.; Ding, T.; Li, T.; Lu, X.; Ho, G.W. Direct-Ink-Write 3D Printing of Hydrogels into Biomimetic Soft Robots. *ACS Nano* **2019**, *13*, 13176–13184. [CrossRef]
105. Pasco, J.; Lei, Z.; Aranas, C. Additive Manufacturing in Off-Site Construction: Review and Future Directions. *Buildings* **2022**, *12*, 53. [CrossRef] [PubMed]
106. Bodaghi, M.; Liao, W.H. 4D Printed Tunable Mechanical Metamaterials with Shape Memory Operations. *Smart Mater. Struct.* **2019**, *28*, 045019. [CrossRef]
107. Alshebly, Y.S.; Nafea, M.; Mustapha, K.B.; Ali, M.S.M.; Mohd Faudzi, A.A.; Tien, M.T.T.; Almurib, H.A. Variable Stiffness 4D Printing. In *Smart Materials in Additive Manufacturing—Volume 2: 4D Printing Mechanics, Modeling, and Advanced Engineering Applications*; Elsevier: Amsterdam, The Netherlands, 2022; pp. 407–433. [CrossRef]
108. Mao, Y.; Yu, K.; Isakov, M.S.; Wu, J.; Dunn, M.L.; Jerry Qi, H. Sequential Self-Folding Structures by 3D Printed Digital Shape Memory Polymers. *Sci. Rep.* **2015**, *5*, 13616. [CrossRef] [PubMed]
109. Herath, M.; Epaarachchi, J.; Islam, M.; Fang, L.; Leng, J. Light Activated Shape Memory Polymers and Composites: A Review. *Eur. Polym. J.* **2020**, *136*, 109912. [CrossRef]
110. Chen, Y.; Chen, C.; Rehman, H.U.; Zheng, X.; Li, H.; Liu, H.; Hedenqvist, M.S. Shape-Memory Polymeric Artificial Muscles: Mechanisms, Applications and Challenges. *Molecules* **2020**, *25*, 4246. [CrossRef]
111. Tan, L.J.; Zhu, W.; Zhou, K. Recent Progress on Polymer Materials for Additive Manufacturing. *Adv. Funct. Mater.* **2020**, *30*, 2003062. [CrossRef]
112. Bao, Y.; Paunović, N.; Leroux, J. Challenges and Opportunities in 3D Printing of Biodegradable Medical Devices by Emerging Photopolymerization Techniques. *Adv. Funct. Mater.* **2022**, *32*, 2109864. [CrossRef]
113. Topa, M.; Ortyl, J. Moving Towards a Finer Way of Light-Cured Resin-Based Restorative Dental Materials: Recent Advances in Photoinitiating Systems Based on Iodonium Salts. *Materials* **2020**, *13*, 4093. [CrossRef] [PubMed]
114. Hoyle, C.E.; Kinstle, J.F. Radiation Curing of Polymeric Materials. *ACSS* **1990**, *417*. [CrossRef]
115. Lalevée, J.; Tehfe, M.A.; Dumur, F.; Gigmes, D.; Graff, B.; Morlet-Savary, F.; Fouassier, J.P. Light-Harvesting Organic Photoinitiators of Polymerization. *Macromol. Rapid Commun.* **2013**, *34*, 239–245. [CrossRef]
116. Fouassier, J.P.; Allonas, X.; Burget, D. Photopolymerization Reactions under Visible Lights: Principle, Mechanisms and Examples of Applications. *Prog. Org. Coat.* **2003**, *47*, 16–36. [CrossRef]
117. Jasinski, F.; Zetterlund, P.B.; Braun, A.M.; Chemtob, A. Photopolymerization in Dispersed Systems. *Prog. Polym. Sci.* **2018**, *84*, 47–88. [CrossRef]
118. Shaukat, U.; Rossegger, E.; Schlögl, S. A Review of Multi-Material 3D Printing of Functional Materials via Vat Photopolymerization. *Polymers* **2022**, *14*, 2449. [CrossRef]
119. Joharji, L.; Mishra, R.B.; Alam, F.; Tytov, S.; Al-Modaf, F.; El-Atab, N. 4D Printing: A Detailed Review of Materials, Techniques, and Applications. *Microelectron. Eng.* **2022**, *265*, 33–36. [CrossRef]

120. Kunio, I.; Takeshi, E. A Review of the Development of Radical Photopolymerization Initiators Used for Designing Light-Curing Dental Adhesives and Resin Composites. *Dent. Mater. J.* **2010**, *29*, 481–501. [CrossRef]
121. Li, A.; Challapalli, A.; Li, G. 4D Printing of Recyclable Lightweight Architectures Using High Recovery Stress Shape Memory Polymer. *Sci. Rep.* **2019**, *9*, 7621. [CrossRef] [PubMed]
122. Ng, C.S.; Subramanian, A.S.; Su, P.C. Zinc Oxide Nanoparticles as Additives for Improved Dimensional Accuracy in Vat Photopolymerization. *Addit. Manuf.* **2022**, *59*, 103118. [CrossRef]
123. Kuang, X.; Zhao, Z.; Chen, K.; Fang, D.; Kang, G.; Qi, H.J. High-speed 3D Printing of High-performance Thermosetting Polymers via Two-stage Curing. *Macromol. Rapid Commun.* **2018**, *39*, 1700809. [CrossRef]
124. Wu, H.; Chen, P.; Yan, C.; Cai, C.; Shi, Y. Four-Dimensional Printing of a Novel Acrylate-Based Shape Memory Polymer Using Digital Light Processing. *Mater. Des.* **2019**, *171*, 107704. [CrossRef]
125. Choong, Y.Y.C.; Maleksaeedi, S.; Eng, H.; Su, P.C.; Wei, J. Curing Characteristics of Shape Memory Polymers in 3D Projection and Laser Stereolithography. *Virtual Phys. Prototyp.* **2017**, *12*, 77–84. [CrossRef]
126. Hassan, R.U.; Jo, S.; Seok, J. Fabrication of a Functionally Graded and Magnetically Responsive Shape Memory Polymer Using a 3D Printing Technique and Its Characterization. *J. Appl. Polym. Sci.* **2018**, *135*, 45997. [CrossRef]
127. Huang, L.; Jiang, R.; Wu, J.; Song, J.; Bai, H.; Li, B.; Zhao, Q.; Xie, T. Ultrafast Digital Printing toward 4D Shape Changing Materials. *Adv. Mater.* **2017**, *29*, 1605390. [CrossRef]
128. Meereis, C.T.W.; Leal, F.B.; Lima, G.S.; De Carvalho, R.V.; Piva, E.; Ogliari, F.A. BAPO as an Alternative Photoinitiator for the Radical Polymerization of Dental Resins. *Dent. Mater.* **2014**, *30*, 945–953. [CrossRef]
129. Han, M.; Zhao, J.; Li, L.; Tan, M. Shape Memory Properties of 4D Printed Parts Under Cyclic Loading: Effects of Infill Characteristics and Stimulus Conditions. In Proceedings of the ASME 2022 17th International Manufacturing Science and Engineering Conference, West Lafayette, IN, USA, 27 June–1 July 2022. [CrossRef]
130. Tang, Z.; Gong, J.; Cao, P.; Tao, L.; Pei, X.; Wang, T.; Zhang, Y.; Wang, Q.; Zhang, J. 3D Printing of a Versatile Applicability Shape Memory Polymer with High Strength and High Transition Temperature. *Chem. Eng. J.* **2022**, *431*, 134211. [CrossRef]
131. Rossegger, E.; Höller, R.; Reisinger, D.; Fleisch, M.; Strasser, J.; Wieser, V.; Griesser, T.; Schlögl, S. High Resolution Additive Manufacturing with Acrylate Based Vitrimers Using Organic Phosphates as Transesterification Catalyst. *Polymer* **2021**, *221*, 123631. [CrossRef]
132. Alabiso, W.; Hron, T.M.; Reisinger, D.; Bautista-Anguís, D.; Schlögl, S. Shape Memory-Assisted Self-Healing of Dynamic Thiol-Acrylate Networks. *Polym. Chem.* **2021**, *12*, 5704–5714. [CrossRef]
133. Cortés, A.; Cosola, A.; Sangermano, M.; Campo, M.; González Prolongo, S.; Pirri, C.F.; Jiménez-Suárez, A.; Chiappone, A. DLP 4D-Printing of Remotely, Modularly, and Selectively Controllable Shape Memory Polymer Nanocomposites Embedding Carbon Nanotubes. *Adv. Funct. Mater.* **2021**, *31*, 2106774. [CrossRef]
134. Park, D.; Lee, S.; Kim, J. Thermoelectric and Mechanical Properties of PEDOT:PSS-Coated Ag_2Se Nanowire Composite Fabricated via Digital Light Processing Based 3D Printing. *Compos. Commun.* **2022**, *30*, 101084. [CrossRef]
135. Rossegger, E.; Höller, R.; Reisinger, D.; Strasser, J.; Fleisch, M.; Griesser, T.; Schlögl, S. Digital Light Processing 3D Printing with Thiol–Acrylate Vitrimers. *Polym. Chem.* **2021**, *12*, 639–644. [CrossRef]
136. Davidson, E.C.; Kotikian, A.; Li, S.; Aizenberg, J.; Lewis, J.A. 3D Printable and Reconfigurable Liquid Crystal Elastomers with Light-Induced Shape Memory via Dynamic Bond Exchange. *Adv. Mater.* **2020**, *32*, 1905682. [CrossRef]
137. Razzaq, M.Y.; Gonzalez-Gutierrez, J.; Mertz, G.; Ruch, D.; Schmidt, D.F.; Westermann, S. 4D Printing of Multicomponent Shape-Memory Polymer Formulations. *Appl. Sci.* **2022**, *12*, 7880. [CrossRef]
138. Tarek Benkhaled, B.; Belkhir, K.; Brossier, T.; Chatard, C.; Graillot, A.; Lonetti, B.; Mingotaud, A.-F.; Catrouillet, S.; Blanquer, S.; Lapinte, V. 3D Fabrication of Shape-Memory Polymer Networks Based on Coumarin Photo-Dimerization. *Eur. Polym. J.* **2022**, *179*, 111570. [CrossRef]
139. Han, M.; Li, L.; Zhao, J. Volatile Organic Compound Emissions from 4D Printing: Effects of Material Composition and External Stimulus. *Addit. Manuf.* **2022**, *56*, 102894. [CrossRef]
140. Zhang, Y.; Huang, L.; Song, H.; Ni, C.; Wu, J.; Zhao, Q.; Xie, T. 4D Printing of a Digital Shape Memory Polymer with Tunable High Performance. *ACS Appl. Mater. Interfaces* **2019**, *11*, 32408–32413. [CrossRef]
141. Han, D.; Morde, R.S.; Mariani, S.; La Mattina, A.A.; Vignali, E.; Yang, C.; Barillaro, G.; Lee, H. 4D Printing of a Bioinspired Microneedle Array with Backward-Facing Barbs for Enhanced Tissue Adhesion. *Adv. Funct. Mater.* **2020**, *30*, 1909197. [CrossRef]
142. Li, X.; Yu, R.; He, Y.; Zhang, Y.; Yang, X.; Zhao, X.; Huang, W. Four-Dimensional Printing of Shape Memory Polyurethanes with High Strength and Recyclability Based on Diels-Alder Chemistry. *Polymer* **2020**, *200*, 122532. [CrossRef]
143. Duan, H.; Leng, K.; Xu, X.; Li, Q.; Liu, D.; Han, Y.; Gao, J.; Yu, Q.; Wang, Z. Monoacylphosphine Oxides with Substituents in the Phosphonyl Moiety as Norrish I Photoinitiators: Synthesis, Photoinitiattion Properties and Mechanism. *J. Photochem. Photobiol. A Chem.* **2021**, *421*, 113517. [CrossRef]
144. Zarek, M.; Mansour, N.; Shapira, S.; Cohn, D. 4D Printing of Shape Memory-Based Personalized Endoluminal Medical Devices. *Macromol. Rapid Commun.* **2017**, *38*, 1600628. [CrossRef]
145. Li, Y.; Zheng, W.; Li, B.; Dong, J.; Gao, G.; Jiang, Z. Double-Layer Temperature-Sensitive Hydrogel Fabricated by 4D Printing with Fast Shape Deformation. *Colloids Surf. A Physicochem. Eng. Asp.* **2022**, *648*, 129307. [CrossRef]

146. Halbardier, L.; Goldbach, E.; Croutx'croutxé-Barghorn, C.; Schuller, A.-S.; Allonas, X. Combined Aza-Michael and Radical Photopolymerization Reactions for Enhanced Mechanical Properties of 3D Printed Shape Memory Polymers. *RSC Adv.* **2022**, *12*, 30381–30385. [CrossRef] [PubMed]
147. Ehrmann, G.; Ehrmann, A. 3D Printing of Shape Memory Polymers. *J. Appl. Polym. Sci.* **2021**, *138*, 50847. [CrossRef]
148. Zhang, W.; Wang, H.; Wang, H.; Chan, J.Y.E.; Liu, H.; Zhang, B.; Zhang, Y.F.; Agarwal, K.; Yang, X.; Ranganath, A.S.; et al. Structural Multi-Colour Invisible Inks with Submicron 4D Printing of Shape Memory Polymers. *Nat. Commun.* **2021**, *12*, 1–8. [CrossRef]
149. Feng, X.; Li, G. High-Temperature Shape Memory Photopolymer with Intrinsic Flame Retardancy and Record-High Recovery Stress. *Appl. Mater. Today* **2021**, *23*, 101056. [CrossRef]
150. Chen, L.; Zhang, Y.; Ye, H.; Duan, G.; Duan, H.; Ge, Q.; Wang, Z. Color-Changeable Four-Dimensional Printing Enabled with Ultraviolet-Curable and Thermochromic Shape Memory Polymers. *ACS Appl. Mater. Interfaces* **2021**, *13*, 18120–18127. [CrossRef]
151. Zhang, H.; Huang, S.; Sheng, J.; Fan, L.; Zhou, J.; Shan, M.; Wei, J.; Wang, C.; Yang, H.; Lu, J. 4D Printing of Ag Nanowire-Embedded Shape Memory Composites with Stable and Controllable Electrical Responsivity: Implications for Flexible Actuators. *ACS Appl. Nano Mater.* **2022**, *5*, 6221–6231. [CrossRef]
152. Launay, V.; Dumur, F.; Gigmes, D.; Lalevée, J. Near-Infrared Light for Polymer Re-Shaping and Re-Processing Applications. *J. Polym. Sci.* **2021**, *59*, 2193–2200. [CrossRef]
153. He, W.; Ming, X.; Xiang, Y.; Zhang, C.; Zhu, H.; Zhang, Q.; Zhu, S. Bioinspired Semicrystalline Dynamic Ionogels with Adaptive Mechanics and Tactile Sensing. *ACS Appl. Mater. Interfaces* **2022**, *14*, 20132–20138. [CrossRef] [PubMed]
154. Gauvin, R.; Chen, Y.C.; Lee, J.W.; Soman, P.; Zorlutuna, P.; Nichol, J.W.; Bae, H.; Chen, S.; Khademhosseini, A. Microfabrication of Complex Porous Tissue Engineering Scaffolds Using 3D Projection Stereolithography. *Biomaterials* **2012**, *33*, 3824–3834. [CrossRef] [PubMed]
155. Le Fer, G.; Becker, M.L. 4D Printing of Resorbable Complex Shape-Memory Poly(Propylene Fumarate) Star Scaffolds. *ACS Appl. Mater. Interfaces* **2020**, *12*, 22444–22452. [CrossRef]
156. Cullen, A.T.; Price, A.D. Digital Light Processing for the Fabrication of 3D Intrinsically Conductive Polymer Structures. *Synth. Met.* **2018**, *235*, 34–41. [CrossRef]
157. Zhao, Z.; Mu, X.; Wu, J.; Qi, H.J.; Fang, D. Effects of Oxygen on Interfacial Strength of Incremental Forming of Materials by Photopolymerization. *Extrem. Mech. Lett.* **2016**, *9*, 108–118. [CrossRef]
158. Jariwala, A.S.; Ding, F.; Boddapati, A.; Breedveld, V.; Grover, M.A.; Henderson, C.L.; Rosen, D.W. Modeling Effects of Oxygen Inhibition in Mask-Based Stereolithography. *Rapid Prototyp. J.* **2011**, *17*, 168–175. [CrossRef]
159. Griffini, G.; Invernizzi, M.; Levi, M.; Natale, G.; Postiglione, G.; Turri, S. 3D-Printable CFR Polymer Composites with Dual-Cure Sequential IPNs. *Polymer* **2016**, *91*, 174–179. [CrossRef]
160. Huang, B.; Wu, B.; Han, L.; Lu, Z.; Zhou, W. Preparation of a Novel Cationic Photosensitive Resin (3D-SLR01) for Stereolithography 3D Printing and Determination of Its Some Properties. *J. Wuhan Univ. Technol. Sci. Ed.* **2019**, *34*, 761–768. [CrossRef]
161. Schwartz, J.J.; Boydston, A.J. Multimaterial Actinic Spatial Control 3D and 4D Printing. *Nat. Commun.* **2019**, *10*, 1–10. [CrossRef]
162. Lai, H.; Zhang, J.; Xing, F.; Xiao, P. Recent Advances in Light-Regulated Non-Radical Polymerisations. *Chem. Soc. Rev.* **2020**, *49*, 1867–1886. [CrossRef]
163. Wang, B.; Engay, E.; Stubbe, P.R.; Moghaddam, S.Z.; Thormann, E.; Almdal, K.; Islam, A.; Yang, Y. Stiffness Control in Dual Color Tomographic Volumetric 3D Printing. *Nat. Commun.* **2022**, *13*, 367. [CrossRef] [PubMed]
164. Yang, C.; Yang, Z.G. Synthesis of Low Viscosity, Fast UV Curing Solder Resist Based on Epoxy Resin for Ink-Jet Printing. *J. Appl. Polym. Sci.* **2013**, *129*, 187–192. [CrossRef]
165. Khorasani, M.; Ghasemi, A.H.; Rolfe, B.; Gibson, I. Additive Manufacturing a Powerful Tool for the Aerospace Industry. *Rapid Prototyp. J.* **2022**, *28*, 87–100. [CrossRef]
166. Al Mousawi, A.; Poriel, C.; Toufaily, J.; Dumur, F.; Hamieh, T.; Pierre Fouassier, J.; Laleveé, J.; Lebanon, B. Zinc Tetraphenylporphyrin as High Performance Visible Light Photoinitiator of Cationic Photosensitive Resins for LED Projector 3D Printing Applications. *ACS Publ.* **2017**, *50*, 746–753. [CrossRef]
167. Subramanian, A.S.; Tey, J.N.; Zhang, L.; Ng, B.H.; Roy, S.; Wei, J.; Hu, X.M. Synergistic Bond Strengthening in Epoxy Adhesives Using Polydopamine/MWCNT Hybrids. *Polymer* **2016**, *82*, 285–294. [CrossRef]
168. Subramanian, A.S.; Hu, X. 'Matthew' Heterogeneous Photosensitizers: Super-Efficient Dual Functional Polydopamine Nanohybrid for Epoxy Photopolymerization. *Polymer* **2022**, *243*, 124558. [CrossRef]
169. Wang, Y.; Sachyani Keneth, E.; Kamyshny, A.; Scalet, G.; Auricchio, F.; Magdassi, S. 4D Multimaterial Printing of Programmable and Selective Light-Activated Shape-Memory Structures with Embedded Gold Nanoparticles. *Adv. Mater. Technol.* **2022**, *7*, 2101058. [CrossRef]
170. Duan, Y.; Zhou, Y.; Tang, Y.; Li, D. Nano-TiODN2/DN-Modified Photosensitive Resin for RP. *Rapid Prototyp. J.* **2011**, *17*, 247–252. [CrossRef]
171. Chen, K.; Kuang, X.; Li, V.; Kang, G.; Qi, H.J. Fabrication of Tough Epoxy with Shape Memory Effects by UV-Assisted Direct-Ink Write Printing. *Soft Matter* **2018**, *14*, 1879–1886. [CrossRef]
172. Lai, H.; Peng, X.; Li, L.; Zhu, D.; Xiao, P. Novel Monomers for Photopolymer Networks. *Prog. Polym. Sci.* **2022**, *128*, 101529. [CrossRef]

173. Bednarczyk, P.; Mozelewska, K.; Nowak, M.; Czech, Z. Photocurable Epoxy Acrylate Coatings Preparation by Dual Cationic and Radical Photocrosslinking. *Materials* **2021**, *14*, 4150. [CrossRef]
174. Noè, C.; Hakkarainen, M.; Sangermano, M. Cationic UV-Curing of Epoxidized Biobased Resins. *Polymers* **2020**, *13*, 89. [CrossRef]
175. Yakacki, C.M.; Willis, S.; Luders, C.; Gall, K. Deformation Limits in Shape-Memory Polymers. *Adv. Eng. Mater.* **2008**, *10*, 112–119. [CrossRef]
176. Radchenko, A.V.; Duchet-Rumeau, J.; Gérard, J.-F.; Baudoux, J.; Livi, S. Cycloaliphatic Epoxidized Ionic Liquids as New Versatile Monomers for the Development of Shape Memory PIL Networks by 3D Printing. *Polym. Chem.* **2020**, *11*, 5475–5483. [CrossRef]
177. Liu, J.; Miao, P.; Zhang, W.; Song, G.; Feng, J.; Leng, X.; Li, Y. Synthesis and Characterization of Interpenetrating Polymer Networks (IPNs) Based on UV Curable Resin and Blocked Isocyanate/Polyols. *Polymer* **2022**, *256*, 125254. [CrossRef]
178. Mallakpour, S.; Tabesh, F.; Hussain, C.M. A New Trend of Using Poly(Vinyl Alcohol) in 3D and 4D Printing Technologies: Process and Applications. *Adv. Colloid Interface Sci.* **2022**, *301*, 102605. [CrossRef]
179. Rahmat-Samii, Y.; Topsakal, E. (Eds.) *Antenna and Sensor Technologies in Modern Medical Applications*; Wiley: Hoboken, NJ, USA, 2021; ISBN 9781119683285.
180. Willemen, N.G.A.; Morsink, M.A.J.; Veerman, D.; da Silva, C.F.; Cardoso, J.C.; Souto, E.B.; Severino, P. From Oral Formulations to Drug-Eluting Implants: Using 3D and 4D Printing to Develop Drug Delivery Systems and Personalized Medicine. *Bio-Design Manuf.* **2022**, *5*, 85–106. [CrossRef]
181. Yilmaz, B.; Al Rashid, A.; Mou, Y.A.; Evis, Z.; Koç, M. Bioprinting: A Review of Processes, Materials and Applications. *Bioprinting* **2021**, *23*, e00148. [CrossRef]
182. Pilipović, A.; Raos, P.; Šercer, M. Experimental Analysis of Properties of Materials for Rapid Prototyping. *Int. J. Adv. Manuf. Technol.* **2009**, *40*, 105–115. [CrossRef]
183. Jeong, H.Y.; Woo, B.H.; Kim, N.; Jun, Y.C. Multicolor 4D Printing of Shape-Memory Polymers for Light-Induced Selective Heating and Remote Actuation. *Sci. Rep.* **2020**, *10*, 6258. [CrossRef] [PubMed]
184. Zhou, K. *Additive Manufacturing Technology: Design, Optimization, and Modeling*; Wiley: Hoboken, NJ, USA, 2022; ISBN 9783527833924.
185. Neagu, A. *Towards 4D Bioprinting*; Elsevier Science: Amsterdam, The Netherlands, 2022; ISBN 9780128187456.
186. Cheng, Y.L.; Huang, K.C. Preparation and Characterization of Color Photocurable Resins for Full-Color Material Jetting Additive Manufacturing. *Polymers* **2020**, *12*, 650. [CrossRef] [PubMed]
187. Ding, Z.; Yuan, C.; Peng, X.; Wang, T.; Qi, H.J.; Dunn, M.L. Direct 4D Printing via Active Composite Materials. *Sci. Adv.* **2017**, *3*, e1602890. [CrossRef] [PubMed]
188. Balani, S.B.; Ghaffar, S.H.; Chougan, M.; Pei, E.; Şahin, E. Processes and Materials Used for Direct Writing Technologies: A Review. *Results Eng.* **2021**, *11*, 100257. [CrossRef]
189. Guo, Y.; Liu, Y.; Liu, J.; Zhao, J.; Zhang, H.; Zhang, Z. Shape Memory Epoxy Composites with High Mechanical Performance Manufactured by Multi-Material Direct Ink Writing. *Compos. Part A Appl. Sci. Manuf.* **2020**, *135*. [CrossRef]
190. Li, X.; Yang, Y.; Zhang, Y.; Wang, T.; Yang, Z.; Wang, Q.; Zhang, X. Dual-Method Molding of 4D Shape Memory Polyimide Ink. *Mater. Des.* **2020**, *191*, 108606. [CrossRef]
191. Chi, H.; Lin, Z.; Chen, Y.; Zheng, R.; Qiu, H.; Hu, X.; Bai, H. Three-Dimensional Printing and Recycling of Multifunctional Composite Material Based on Commercial Epoxy Resin and Graphene Nanoplatelet. *ACS Appl. Mater. Interfaces* **2022**, *14*, 13758–13767. [CrossRef]
192. Idowu, A.; Thomas, T.; Boesl, B.; Agarwal, A. Cryo-Assisted Extrusion 3D Printing of Shape Memory Polymer-Graphene Composites. *J. Manuf. Sci. Eng.* **2022**, *145*, 1–17. [CrossRef]
193. Bodkhe, S.; Ermanni, P. 3D Printing of Multifunctional Materials for Sensing and Actuation: Merging Piezoelectricity with Shape Memory. *Eur. Polym. J.* **2020**, *132*, 109738. [CrossRef]
194. Wan, X.; Luo, L.; Liu, Y.; Leng, J. Direct Ink Writing Based 4D Printing of Materials and Their Applications. *Adv. Sci.* **2020**, *7*, 2001000. [CrossRef]
195. Compton, B.G.; Hmeidat, N.S.; Pack, R.C.; Heres, M.F.; Sangoro, J.R. Electrical and Mechanical Properties of 3D-Printed Graphene-Reinforced Epoxy. *JOM* **2018**, *70*, 292–297. [CrossRef]
196. Lewicki, J.P.; Rodriguez, J.N.; Zhu, C.; Worsley, M.A.; Wu, A.S.; Kanarska, Y.; Horn, J.D.; Duoss, E.B.; Ortega, J.M.; Elmer, W.; et al. 3D-Printing of Meso-Structurally Ordered Carbon Fiber/Polymer Composites with Unprecedented Orthotropic Physical Properties. *Sci. Rep.* **2017**, *7*, 43401. [CrossRef] [PubMed]
197. Rodriguez, J.N.; Zhu, C.; Duoss, E.B.; Wilson, T.S.; Spadaccini, C.M.; Lewicki, J.P. Shape-Morphing Composites with Designed Micro-Architectures. *Sci. Rep.* **2016**, *6*, 27933. [CrossRef]
198. Pandey, H.; Mohol, S.S.; Kandi, R. 4D Printing of Tracheal Scaffold Using Shape-Memory Polymer Composite. *Mater. Lett.* **2022**, *329*, 133238. [CrossRef]
199. Wan, X.; Wei, H.; Zhang, F.-H.; Liu, Y.; Leng, J. 3D Printing of Shape Memory Poly(d,l-Lactide-Co-Trimethylene Carbonate) by Direct Ink Writing for Shape-Changing Structures. *J. Appl. Polym. Sci.* **2019**, *136*, 48177. [CrossRef]
200. Wang, Y.J.; Jeng, U.S.; Hsu, S.H. Biodegradable Water-Based Polyurethane Shape Memory Elastomers for Bone Tissue Engineering. *ACS Biomater. Sci. Eng.* **2018**, *4*, 1397–1406. [CrossRef]
201. Yamagishi, K.; Zhou, W.; Ching, T.; Huang, S.Y.; Hashimoto, M. Ultra-Deformable and Tissue-Adhesive Liquid Metal Antennas with High Wireless Powering Efficiency. *Adv. Mater.* **2021**, *33*, 2008062. [CrossRef]

202. Park, Y.; Yun, I.; Chung, W.G.; Park, W.; Lee, D.H.; Park, J. High-Resolution 3D Printing for Electronics. *Adv. Sci.* **2022**, *9*, 2104623. [CrossRef] [PubMed]
203. Chen, M.; Gao, M.; Bai, L.; Zheng, H.; Qi, H.J.; Zhou, K. Recent Advances in 4D Printing of Liquid Crystal Elastomers. *Adv. Mater.* **2022**, *9*, 2209566. [CrossRef]
204. Del Pozo, M.; Sol, J.A.H.P.; Schenning, A.P.H.J.; Debije, M.G. 4D Printing of Liquid Crystals: What's Right for Me? *Adv. Mater.* **2022**, *34*, 2104390. [CrossRef] [PubMed]
205. Xiao, Y.Y.; Jiang, Z.C.; Hou, J.B.; Chen, X.S.; Zhao, Y. Electrically Driven Liquid Crystal Network Actuators. *Soft Matter* **2022**, *18*, 4850–4867. [CrossRef]
206. Liu, K.; Hacker, F.; Daraio, C. Robotic Surfaces with Reversible, Spatiotemporal Control for Shape Morphing and Object Manipulation. *Sci. Robot.* **2021**, *6*, eabf5116. [CrossRef] [PubMed]
207. Roach, D.J.; Sun, X.; Peng, X.; Demoly, F.; Zhou, K.; Qi, H.J. 4D Printed Multifunctional Composites with Cooling-Rate Mediated Tunable Shape Morphing. *Adv. Funct. Mater.* **2022**, *32*, 2203236. [CrossRef]
208. Wang, C.; Sim, K.; Chen, J.; Kim, H.; Rao, Z.; Li, Y.; Chen, W.; Song, J.; Verduzco, R.; Yu, C. Soft Ultrathin Electronics Innervated Adaptive Fully Soft Robots. *Adv. Mater.* **2018**, *30*, 1870087. [CrossRef]
209. Long, F.; Xu, G.; Wang, J.; Ren, Y.; Cheng, Y. Variable Stiffness Conductive Composites by 4D Printing Dual Materials Alternately. *Micromachines* **2022**, *13*, 1343. [CrossRef]
210. Kotikian, A.; Truby, R.L.; Boley, J.W.; White, T.J.; Lewis, J.A. 3D Printing of Liquid Crystal Elastomeric Actuators with Spatially Programed Nematic Order. *Adv. Mater.* **2018**, *30*, 1706164. [CrossRef] [PubMed]
211. Kotikian, A.; McMahan, C.; Davidson, E.C.; Muhammad, J.M.; Weeks, R.D.; Daraio, C.; Lewis, J.A. Untethered Soft Robotic Matter with Passive Control of Shape Morphing and Propulsion. *Sci. Robot.* **2019**, *4*. [CrossRef]
212. Mistry, D.; Traugutt, N.A.; Sanborn, B.; Volpe, R.H.; Chatham, L.S.; Zhou, R.; Song, B.; Yu, K.; Long, K.N.; Yakacki, C.M. Soft Elasticity Optimises Dissipation in 3D-Printed Liquid Crystal Elastomers. *Nat. Commun.* **2021**, *12*, 1–10. [CrossRef]
213. Dumanli, A.G.; Savin, T. Recent Advances in the Biomimicry of Structural Colours. *Chem. Soc. Rev.* **2016**, *45*, 6698–6724. [CrossRef]
214. Scarangella, A.; Soldan, V.; Mitov, M. Biomimetic Design of Iridescent Insect Cuticles with Tailored, Self-Organized Cholesteric Patterns. *Nat. Commun.* **2020**, *11*, 4108. [CrossRef]
215. López-Valdeolivas, M.; Liu, D.; Broer, D.J.; Sánchez-Somolinos, C. 4D Printed Actuators with Soft-Robotic Functions. *Macromol. Rapid Commun.* **2018**, *39*, 1700710. [CrossRef]
216. Kamal, A.; Ashmawy, M.; Algazzar, A.M.; Elsheikh, A.H. Fabrication Techniques of Polymeric Nanocomposites: A Comprehensive Review. *Proc. Inst. Mech. Eng. Part C J. Mech. Eng. Sci.* **2022**, *236*, 4843–4861. [CrossRef]
217. Weng, Z.; Wang, J.; Senthil, T.; Wu, L. Mechanical and Thermal Properties of ABS/Montmorillonite Nanocomposites for Fused Deposition Modeling 3D Printing. *Mater. Des.* **2016**, *102*, 276–283. [CrossRef]
218. Alsaadi, M.; Younus, B.; Erklig, A.; Bulut, M.; Bozkurt, O.; Sulaiman, B. Effect of Graphene Nano-Platelets on Mechanical and Impact Characteristics of Carbon/Kevlar Reinforced Epoxy Hybrid Nanocomposites. *Proc. Inst. Mech. Eng. Part C J. Mech. Eng. Sci.* **2021**, *235*, 7139–7151. [CrossRef]
219. Pollack, S.; Venkatesh, C.; Neff, M.; Healy, A.V.; Hu, G.; Fuenmayor, E.A.; Lyons, J.G.; Major, I.; Devine, D.M. Polymer-Based Additive Manufacturing: Historical Developments, Process Types and Material Considerations. In *Polymer-Based Additive Manufacturing*; Springer International Publishing: Cham, Switzerland, 2019; pp. 1–22.
220. Singh, P.; Srivastava, S.; Singh, S.K. Nanosilica: Recent Progress in Synthesis, Functionalization, Biocompatibility, and Biomedical Applications. *ACS Biomater. Sci. Eng.* **2019**, *5*, 4882–4898. [CrossRef]
221. Shen, X.; Wang, Z.; Wu, Y.; Liu, X.; Kim, J.-K. Effect of Functionalization on Thermal Conductivities of Graphene/Epoxy Composites. *Carbon* **2016**, *108*, 412–422. [CrossRef]
222. Naeem, M.; Kuan, H.-C.; Michelmore, A.; Meng, Q.; Qiu, A.; Aakyiir, M.; Losic, D.; Zhu, S.; Ma, J. A New Method for Preparation of Functionalized Graphene and Its Epoxy Nanocomposites. *Compos. Part B Eng.* **2020**, *196*, 108096. [CrossRef]
223. Azlin, M.N.M.; Ilyas, R.A.; Zuhri, M.Y.M.; Sapuan, S.M.; Harussani, M.M.; Sharma, S.; Nordin, A.H.; Nurazzi, N.M.; Afiqah, A.N. 3D Printing and Shaping Polymers, Composites, and Nanocomposites: A Review. *Polymers* **2022**, *14*, 180. [CrossRef]
224. Wu, H.; Fahy, W.P.; Kim, S.; Kim, H.; Zhao, N.; Pilato, L.; Kafi, A.; Bateman, S.; Koo, J.H. Recent Developments in Polymers/Polymer Nanocomposites for Additive Manufacturing. *Prog. Mater. Sci.* **2020**, *111*, 1–10. [CrossRef]
225. Sliozberg, Y.R.; Kröger, M.; Henry, T.C.; Datta, S.; Lawrence, B.D.; Hall, A.J.; Chattopadhyay, A. Computational Design of Shape Memory Polymer Nanocomposites. *Polymer* **2021**, *217*, 123476. [CrossRef]
226. Weng, Z.; Zhou, Y.; Lin, W.; Senthil, T.; Wu, L. Structure-Property Relationship of Nano Enhanced Stereolithography Resin for Desktop SLA 3D Printer. *Compos. Part A Appl. Sci. Manuf.* **2016**, *88*, 234–242. [CrossRef]
227. Zhang, C.; Cui, Y.; Li, J.; Jiang, D. Nano-Sio2-Reinforced Ultraviolet-Curing Materials for Three-Dimensional Printing. *J. Appl. Polym. Sci.* **2015**, *132*. [CrossRef]
228. Gurr, M.; Hofmann, D.; Ehm, M.; Thomann, Y.; Kubier, R.; Mülhaupt, R. Acrylic Nanocomposite Resins for Use in Stereolithography and Structural Light Modulation Based Rapid Prototyping and Rapid Manufacturing Technologies. *Adv. Funct. Mater.* **2008**, *18*, 2390–2397. [CrossRef]
229. Chiu, S.H.; Wu, D.C. Preparation and Physical Properties of Photopolymer/SiO_2 Nanocomposite for Rapid Prototyping System. *J. Appl. Polym. Sci.* **2008**, *107*, 3529–3534. [CrossRef]

230. Cheng, Q.; Zheng, Y.; Wang, T.; Sun, D.; Lin, R. Yellow Resistant Photosensitive Resin for Digital Light Processing 3D Printing. *J. Appl. Polym. Sci.* **2020**, *137*, 48369. [CrossRef]
231. Subramanian, A.S.; Peng, E.; Lau, W.C.; Goh, D.C.W.; Pramono, S.; Sriramulu, D.; Wu, Y.; Kobayashi, H.; Moo, J.G.S.; Su, P.C. Morphological Effects of Various Silica Nanostructures on the Mechanical Properties of Printed Parts in Digital Light Projection 3D Printing. *ACS Appl. Nano Mater.* **2021**, *4*, 4522–4531. [CrossRef]
232. Zhou, L.Y.; Gao, Q.; Fu, J.Z.; Chen, Q.Y.; Zhu, J.P.; Sun, Y.; He, Y. Multimaterial 3D Printing of Highly Stretchable Silicone Elastomers. *ACS Appl. Mater. Interfaces* **2019**, *11*, 23573–23583. [CrossRef]
233. Chen, C.; Justice, R.S.; Schaefer, D.W.; Baur, J.W. Highly Dispersed Nanosilica–Epoxy Resins with Enhanced Mechanical Properties. *Polymer* **2008**, *49*, 3805–3815. [CrossRef]
234. Tian, Y.; Zhang, H.; Zhang, Z. Influence of Nanoparticles on the Interfacial Properties of Fiber-Reinforced-Epoxy Composites. *Compos. Part A Appl. Sci. Manuf.* **2017**, *98*, 1–8. [CrossRef]
235. Alsaadi, M.; Bulut, M.; Erkliğ, A.; Jabbar, A. Nano-Silica Inclusion Effects on Mechanical and Dynamic Behavior of Fiber Reinforced Carbon/Kevlar with Epoxy Resin Hybrid Composites. *Compos. Part B Eng.* **2018**, *152*, 169–179. [CrossRef]
236. Eng, H.; Maleksaeedi, S.; Yu, S.; Choong, Y.Y.C.; Wiria, F.E.; Tan, C.L.C.; Su, P.C.; Wei, J. 3D Stereolithography of Polymer Composites Reinforced with Orientated Nanoclay. *Procedia Eng.* **2017**, *216*, 1–7. [CrossRef]
237. Hmeidat, N.S.; Kemp, J.W.; Compton, B.G. High-Strength Epoxy Nanocomposites for 3D Printing. *Compos. Sci. Technol.* **2018**, *160*, 9–20. [CrossRef]
238. Alsaadi, M.; Erkliğ, A.; Abbas, M. Effect of Clay Nanoparticles on the Mechanical and Vibration Characteristics of Intraply Aramid/Carbon Fiber Reinforced Epoxy Composite. *Polym. Compos.* **2020**, *41*, 2704–2712. [CrossRef]
239. Bulut, M.; Alsaadi, M.; Erkliğ, A. The Effects of Nanosilica and Nanoclay Particles Inclusions on Mode II Delamination, Thermal and Water Absorption of Intraply Woven Carbon/Aramid Hybrid Composites. *Int. Polym. Process.* **2020**, *35*, 367–375. [CrossRef]
240. Mao, Y.; Ding, Z.; Yuan, C.; Ai, S.; Isakov, M.; Wu, J.; Wang, T.; Dunn, M.L.; Qi, H.J. 3D Printed Reversible Shape Changing Components with Stimuli Responsive Materials. *Sci. Rep.* **2016**, *6*, 24761. [CrossRef]
241. Tran, T.S.; Balu, R.; Mettu, S.; Roy Choudhury, N.; Dutta, N.K. 4D Printing of Hydrogels: Innovation in Material Design and Emerging Smart Systems for Drug Delivery. *Pharmaceuticals* **2022**, *15*, 1282. [CrossRef]
242. Anzar, N.; Hasan, R.; Tyagi, M.; Yadav, N.; Narang, J. Carbon Nanotube—A Review on Synthesis, Properties and Plethora of Applications in the Field of Biomedical Science. *Sensors Int.* **2020**, *1*, 100003. [CrossRef]
243. Ma, P.-C.; Siddiqui, N.A.; Marom, G.; Kim, J.-K. Dispersion and Functionalization of Carbon Nanotubes for Polymer-Based Nanocomposites: A Review. *Compos. Part A Appl. Sci. Manuf.* **2010**, *41*, 1345–1367. [CrossRef]
244. Zhang, Y.; Li, H.; Yang, X.; Zhang, T.; Zhu, K.; Si, W.; Liu, Z.; Sun, H. Additive Manufacturing of Carbon Nanotube-Photopolymer Composite Radar Absorbing Materials. *Polym. Compos.* **2018**, *39*, E671–E676. [CrossRef]
245. Mohd Nurazzi, N.; Asyraf, M.R.M.; Khalina, A.; Abdullah, N.; Sabaruddin, F.A.; Kamarudin, S.H.; Ahmad, S.; Mahat, A.M.; Lee, C.L.; Aisyah, H.A.; et al. Fabrication, Functionalization, and Application of Carbon Nanotube-Reinforced Polymer Composite: An Overview. *Polymers* **2021**, *13*, 1047. [CrossRef]
246. Tiwari, S.K.; Sahoo, S.; Wang, N.; Huczko, A. Graphene Research and Their Outputs: Status and Prospect. *J. Sci. Adv. Mater. Devices* **2020**, *5*, 10–29. [CrossRef]
247. Kumar, A.; Sharma, K.; Dixit, A.R. A Review of the Mechanical and Thermal Properties of Graphene and Its Hybrid Polymer Nanocomposites for Structural Applications. *J. Mater. Sci.* **2019**, *54*, 5992–6026. [CrossRef]
248. Huang, X.; Panahi-Sarmad, M.; Dong, K.; Li, R.; Chen, T.; Xiao, X. Tracing Evolutions in Electro-Activated Shape Memory Polymer Composites with 4D Printing Strategies: A Systematic Review. *Compos. Part A Appl. Sci. Manuf.* **2021**, *147*, 106444. [CrossRef]
249. Uysal, E.; Çakir, M.; Ekici, B. Graphene Oxide/Epoxy Acrylate Nanocomposite Production via SLA and Importance of Graphene Oxide Surface Modification for Mechanical Properties. *Rapid Prototyp. J.* **2021**, *27*, 682–691. [CrossRef]
250. Wang, D.; Huang, X.; Li, J.; He, B.; Liu, Q.; Hu, L.; Jiang, G. 3D Printing of Graphene-Doped Target for "Matrix-Free" Laser Desorption/Ionization Mass Spectrometry. *Chem. Commun.* **2018**, *54*, 2723–2726. [CrossRef]
251. Chowdhury, J.; Anirudh, P.V.; Karunakaran, C.; Rajmohan, V.; Mathew, A.T.; Koziol, K.; Alsanie, W.F.; Kannan, C.; Balan, A.S.S.; Thakur, V.K. 4D Printing of Smart Polymer Nanocomposites: Integrating Graphene and Acrylate Based Shape Memory Polymers. *Polymers* **2021**, *13*, 3660. [CrossRef]
252. Kumar, S.; Hofmann, M.; Steinmann, B.; Foster, E.J.; Weder, C. Reinforcement of Stereolithographic Resins for Rapid Prototyping with Cellulose Nanocrystals. *ACS Appl. Mater. Interfaces* **2012**, *4*, 5399–5407. [CrossRef]
253. Lee, D.; Kim, B.-Y.; Park, C.H.; Jeong, G.; Park, S.-D.; Yoo, M.J.; Yang, H.; Lee, W.S. Photocurable Three-Dimensional Printing Resin to Enable Laser-Assisted Selective Electroless Metallization for Customized Electronics. *ACS Appl. Polym. Mater.* **2021**, *3*, 4735–4745. [CrossRef]
254. Krivec, M.; Roshanghias, A.; Abram, A.; Binder, A. Exploiting the Combination of 3D Polymer Printing and Inkjet Ag-Nanoparticle Printing for Advanced Packaging. *Microelectron. Eng.* **2017**, *176*, 1–5. [CrossRef]
255. Ikram, H.; Al Rashid, A.; Koç, M. Synthesis, Characterization, and 3D Printing of Silver Nanoparticles/Photopolymer Resin Composites. *IOP Conf. Ser. Mater. Sci. Eng.* **2022**, *1248*, 012003. [CrossRef]
256. Zhao, J.; Li, Q.; Jin, F.; He, N. Digital Light Processing 3D Printing Kevlar Composites Based on Dual Curing Resin. *Addit. Manuf.* **2021**, *41*, 101962. [CrossRef]

257. Invernizzi, M.; Natale, G.; Levi, M.; Turri, S.; Griffini, G. UV-Assisted 3D Printing of Glass and Carbon Fiber-Reinforced Dual-Cure Polymer Composites. *Materials* **2016**, *9*, 583. [CrossRef] [PubMed]
258. Zhou, Y.; Wang, F.; Yang, Z.; Hu, X.; Pan, Y.; Lu, Y.; Jiang, M. 3D Printing of Polyurethane/Nanocellulose Shape Memory Composites with Tunable Glass Transition Temperature. *Ind. Crops Prod.* **2022**, *182*, 114831. [CrossRef]